Journal of Archaeological Science: Reports 49 (2023) 104011

Contents lists available at ScienceDirect

Journal of Archaeological Science: Reports

journal homepage: www.elsevier.com/locate/jasrep

The obsidian sources of eastern Turkey and the Caucasus: Geochemistry, geology, and geochronology

Ellery Frahm [a,b]

[a] Council on Archaeological Studies and Department of Anthropology, Yale University, New Haven, Connecticut, United States
[b] Anthropology Division, Yale Peabody Museum of Natural History, New Haven, CT, United States

ARTICLE INFO

Keywords:
Southwest Asia
Armenia
Azerbaijan
Georgia
Russia
Turkey
Obsidian sourcing

ABSTRACT

It has been 25 years since the publication of the monograph *L'obsidienne au Proche et Moyen Orient: Du volcan à l'outil* (Cauvin et al., 1998) and, within it, Poidevin's (1998) chapter that summarized all available geochemical and geochronological data for obsidian sources in Turkey and the Caucasus. It was a highly valuable resource to those of us working on Near Eastern obsidian sourcing in the early 2000s; however, an update is long overdue. Poidevin (1998) compiled 229 analyses for obsidian sources in eastern Turkey and the Caucasus, and while he recognized the importance of independent analytical data, he was also frustrated that the few available data obscured real differences in obsidian composition versus variation among the different analytical facilities. Today we are closer to Poidevin's (1998) goal. Here I summarize more than 7300 elemental analyses for 58 geochemically distinct obsidian sources. For example, Poidevin (1998) had just two analyses for Meydan Dağ, a highly important obsidian source, whereas here I report consensus values for 22 elements in Meydan Dağ obsidian based on 423 analyses from 25 independent techniques and laboratories. Not all 58 of the known obsidian sources within this region, however, have been so well characterized, and it is clear that there remains work to be done.

1. Introduction

In 1998, the monograph *L'obsidienne au Proche et Moyen Orient: Du volcan à l'outil* (*Obsidian in the Near and Middle East: From Volcano to Tool*; edited by Cauvin et al., 1998) was published by British Archaeological Reports in their trademark bright red cover. The 388-page volume presented the state-of-the-art regarding knowledge of obsidian in Southwestern Asia at the time, covering topics ranging from the volcanic creation of obsidian to the symbolism of Mesopotamian obsidian artifacts. Those of us who were working on Near Eastern obsidian sourcing in the early 2000s affectionately referred to the book as "The Big Red Bible" of our field. As a doctoral student, I could not afford my own copy of the book, and I had to photocopy one borrowed via Interlibrary Loan. Among the book's sixteen chapters was a 99-page one, written by Jean-Louis Poidevin, titled "Les gisements d'obsidienne de Turquie et de Transcaucasie: géologie, géochimie et chronométrie" (i.e., "The obsidian deposits of Turkey and Transcaucasia: geology, geochemistry, and chronometry"). In his chapter, Poidevin (1998) summarized nearly all that was known of Near Eastern obsidian sources as of the 1990s. That information included a compilation of previously published and unpublished elemental data, including his own measurements, for the obsidian sources as they were understood at the time. The appendix of elemental values was a full 36 pages in length, and it served as a valuable resource for archaeologists, geologists, and analytical chemists interested to match Near Eastern obsidian artifacts to their volcanic origins with such data. It was also one of the few papers to list measurements from neutron activation analysis (NAA), X-ray fluorescence (XRF), and varied forms of inductively coupled plasma (ICP) spectrometry, conducted in a range of analytical facilities around the world, side-by-side for the very same obsidian sources. This, too, was valuable. As noted by Hancock and Carter (2010: 245), "although analytical chemistry is not a democratic process, the agreement of specific elemental concentration data between (among) independent analytical techniques adds credibility" that the datasets are accurate, and ideally, it allows us to arrive at consensus values.

This year marks the 25th anniversary of the monograph and Poidevin's database, and there has been much progress toward a better understanding of the region's obsidian sources. Here I endeavor to provide an update to Poidevin's chapter. Astute readers will realize that this article's title is intended as an homage to that of Poidevin (1998). There are, though, a few differences. For instance, "*Trans*caucasia" and "the *Trans*caucasus" are Russia-centric terms – only from a Russian

E-mail address: ellery.frahm@yale.edu.

https://doi.org/10.1016/j.jasrep.2023.104011
Received 30 January 2023; Received in revised form 4 April 2023; Accepted 12 April 2023
Available online 21 April 2023

perspective do the former Soviet republics of Armenia, Azerbaijan, and Georgia lie "beyond" the Greater Caucasus mountain peaks. Also I list "geochemistry" first in the title because a core focus of this work has been endeavoring to calculate consensus values for elemental concentrations useful for obsidian sourcing. Most notably, eastern Turkey is specified in the title. Here I focus on the obsidian-producing volcanism associated with the Caucasian segment of the vast Alpine–Himalayan collisional belt (Fig. 1). This largely contiguous segment (Fig. 2) and its surroundings, where the Arabian tectonic plate collides with the Eurasian one, have been described by a wide variety of geographic, geological, and topographic names, from the Armenian Highlands and the Southern Caucasus to the Caucasian-Arabian Syntaxis (Sharkov et al., 2015) or even the "Van-Azerbaijan-Armenian SSR" (abbreviated as VAA) by Renfrew and Dixon (1976). This region is distinct from the Central Anatolian Volcanic Province (CAVP) in central Turkey, where the Cappadocian obsidian sources occur, and it is generally less studied. Dixon (1976: 289), one of the original developers of obsidian sourcing, observed that the "extent of our basic geological knowledge decreases from west to east through the… obsidian source" areas from the Western Mediterranean region into the Caucasus, and this held true for Poidevin (1998) too: he listed outcrop-by-outcrop analytical data for the Cappadocian obsidian sources, while he grouped several Caucasus sources together under the heading of "Divers Arménie" (Various Armenian). Given the decades of prior obsidian research in Cappadocia, from the largely unpublished 1970s surveys of Sebastian Payne (see Todd, 1980) to more recent work (Binder et al., 2011), there are more data to organize, summarize, reduce, reconcile, etc. for the obsidian sources in central Turkey. Consequently, the obsidian sources in Cappadocia (and a few minor sources farther to the west; e.g., Yağlar, Orta, Sakaeli) warrant a separate publication, and I focus here only on the sources in eastern Turkey and southwestern Russia as well as the former Soviet republics of Armenia, Azerbaijan, and Georgia.

I wish to emphasize that this paper aims to be comprehensive but not authoritative. Choices (as documented in Section 2) had to be made in creating this database, and I do not necessarily expect that all of my friends and colleagues in this field will concur with each and every one of my choices here, even though those decisions are based on two decades of research. In his chapter, Poidevin (1998) compiled 229 analyses for obsidian sources in eastern Turkey and the Caucasus. Poidevin (1998) emphasized, on one hand, the importance of analytical data collected from independent analytical labs and techniques, but on the other hand, he was frustrated that the few data available at that time confounded efforts to separate actual differences in obsidian composition from variability among analytical facilities. Here, 25 years after Poidevin (1998), I summarize more than 7300 analyses for 58 geochemically distinct obsidian sources. That is, in this region alone, there are more than double the ca. 25 obsidian sources that Keller and Seifried (1990) believed there to be in all of Turkey and the Caucasus. The amount of data available today moves the field much closer to what Poidevin (1998) envisioned. For example, Poidevin (1998) had only two elemental analyses (one from Keller and Seifried, 1990; another from Matsuda, 1990) for one of the most archaeologically important Southwest Asian obsidian sources: Meydan Dağ. In contrast, here I calculate consensus values for Meydan Dağ obsidian using 423 measurements made by 25 independent analytical techniques and laboratories. While Poidevin (1998) included such data as an appendix, here I include them as the modern equivalent: tables in the supplementary materials, which permits a greater degree of custom formatting. This endeavor has been possible by researchers in this field systematically reporting their own source data, such as the recent contribution by Orange et al. (2021) of laser-ablation ICP mass spectrometry (LA-ICP-MS) and portable XRF (pXRF) data from their instruments. As established here, however, some obsidian sources have been analyzed in only one or two laboratories, while other sources have been "hiding" in decades-old datasets all along. Therefore, while I cover the current state-of-the-field, there remains work to be done, as is demonstrated here too.

2. Methods

In this section, I describe the organizing principles that I employed to assemble more than 7300 published and unpublished analyses and to use them to determine consensus values for 22 elements in 58 obsidian sources. Like other researchers who have endeavored to document, describe, and summarize some or all of the obsidian sources in the region (e.g., Blackman, 1984; Keller and Seifried, 1990; Keller et al., 1996; Blackman et al., 1998; Chataigner et al., 1998; Poidevin, 1998; Badalyan

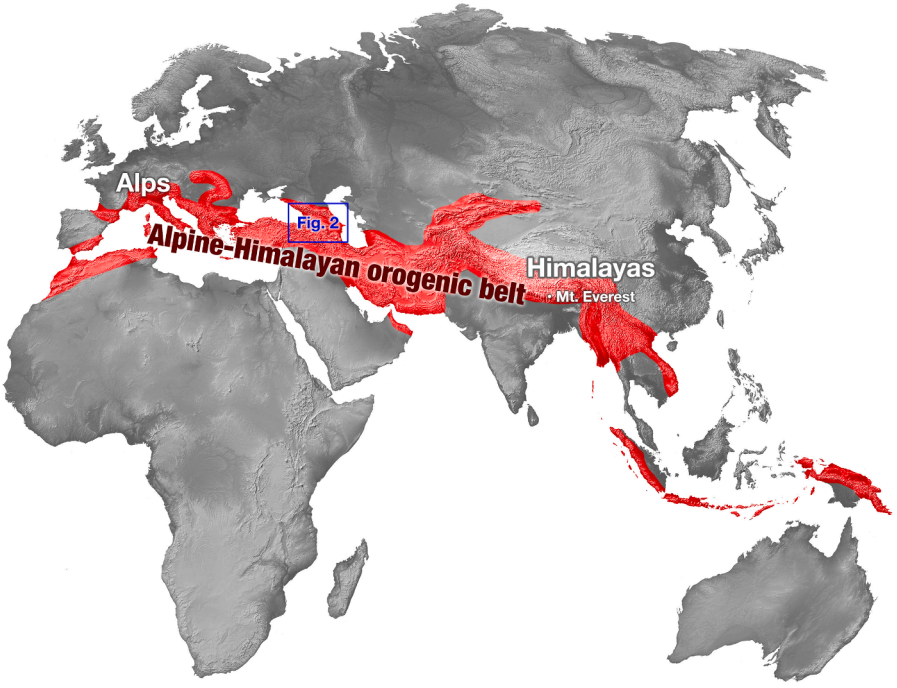

Fig. 1. Topographic map of the eastern hemisphere, highlighting the Alpine-Himalayan orogenic belt.

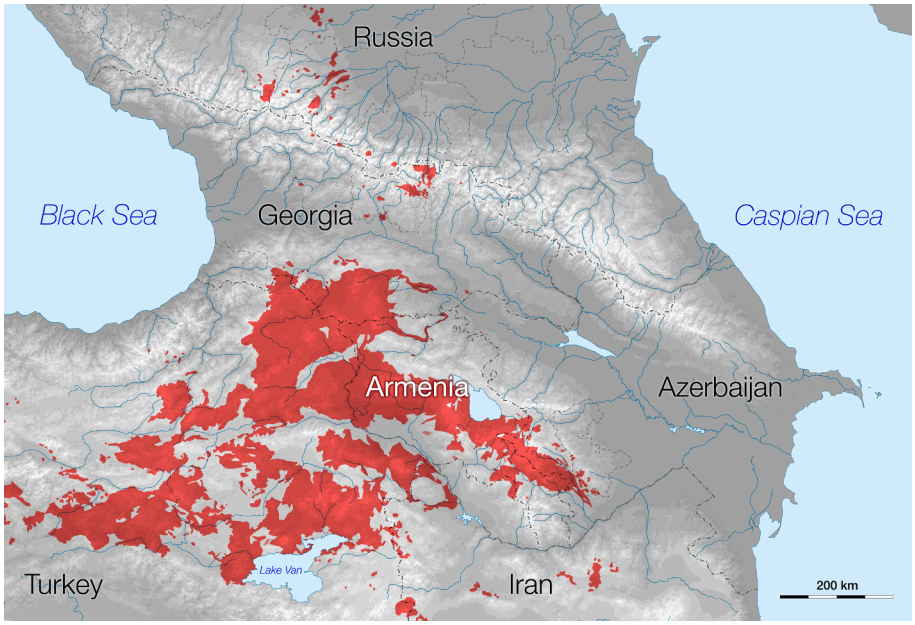

Fig. 2. Topographic map of the study area, highlighting areas of Miocene, Pliocene, and Quaternary (i.e., from 23 Ma to the present) volcanism in the Caucasian segment of the Alpine-Himalayan orogenic belt. Based on and redrawn from Fig. 1. of Lebedev et al. (2013).

et al., 2004; Chataigner and Gratuze, 2014; Orange et al., 2021), I have attempted here to capture the current state-of-the-field for the benefit of not only current archaeologists but also future ones.

I must start with the clarification of an important term: source. Specifically, in the Introduction, I refer to "58 geochemically distinct obsidian sources" in the region of interest. In the obsidian literature, two different usages of "source" can be found: first, the geographic use (i.e., location in space where the obsidian deposit occurs and where past peoples collected the material) and the geochemical use (i.e., a cluster in elemental data, sometimes called a "chemical group"). In brief, the first one can be placed on a map, while the second one can be placed on a compositional scatterplot. Some archaeological scientists prefer the former usage (e.g. Hughes, 1998; Wilson and Pollard, 2001), whereas others prefer the latter (e.g., Harbottle, 1982; Neff, 1998). For the purposes of this article, which principally focuses on deriving consensus elemental ranges for obsidian sources, I favor the usage of fellow obsidian specialist Richard Hughes (1998: 104), who pointed out that "sources are defined, geochemically speaking, on the basis of chemical composition – not spatial distribution." That is, I use the geochemical definition of an obsidian "source" here, synonymous with what some authors might call a "chemical group" or "chemical type" of obsidian. As discussed below in Section 3, not all volcanic origins of obsidian in this region are known, so it would be more challenging to use the geographic definition of a source.

The elemental values for each obsidian source came from (1) data previously published by other researchers and (2) published and unpublished data for obsidian specimens that I either analyzed myself or sent to another facility for analysis. The previously published data were collected during an extensive search of the archaeological, geological, and analytical literature. Data for both geological specimens and sourced artifacts were assembled. Some authors listed the individual analyses, whereas others provided summary statistics (i.e., means and standard deviations). In general, earlier publications include tables in the main manuscript, whereas more recent ones often provide individual analyses in the supplementary materials. Here the summary table for each obsidian source (as listed in Table 1 and discussed in Section 3) includes full citations for all of the publications that contributed data.

Published and unpublished data from my own research are also organized (or re-organized) and shared here, and the elemental data here should be considered to supersede previous work, especially Frahm (2010), in which there were some sampling and/or handling errors that led to incorrect specimen labels before receiving them. Elemental characterization conducted myself involved electron microprobe analysis (EMPA), which is wavelength-dispersive X-ray spectrometry (WDS) conducted inside a scanning electron microscope (SEM), and portable XRF (pXRF), which is energy-dispersive XRF (EDXRF) placed in a small form factor. EMPA was conducted in the Electron Microprobe Laboratory, Department of Earth and Environmental Sciences, University of Minnesota-Twin Cities, and my procedures, including methods of calibration and accuracy assessment, are documented succinctly in Frahm (2020: 6–8) and with greater detail in Frahm (2010: 302–364). Nearly all of my pXRF data were collected using an Olympus Vanta VMR instrument in the Yale University Archaeological Laboratories (e.g., Frahm and Brody, 2019; Frahm and Tryon, 2019) using the Peabody–Yale Reference Obsidians (PYRO) calibration (Frahm, 2019). Some pXRF analyses conducted in Armenia, though, used a Thermo Niton 950 XL3t GOLDD + instrument (e.g., Frahm et al., 2021) calibrated with an early version of the PYRO sets (Frahm, 2019). A portion of my geological specimens were also sent for analysis in other laboratories. At the Missouri University Research Reactor (MURR) Archaeometry Laboratory, specimens were analyzed by NAA using their standard procedures for obsidian (Glascock, 2011) and by EDXRF using either an older ElvaX instrument (Glascock, 2011) or newer Thermo Scientific ARL Quant'X model (Maziar and Glascock, 2017). At the Northwest Research Obsidian Studies Laboratory (NWROSL), specimens were analyzed using a Thermo QuantX-EC EDXRF instrument, and wavelength-dispersive XRF (WDXRF) was conducted using a Bruker/Siemens SRS3000 system in the University of Wisconsin-Eau Claire's (UWEC) Materials Science Center.

Initially the data for 41 elements (Na, Mg, Al, Si, K, Ca, Sc, Ti, V, Cr, Mn, Fe, Ni, Cu, Zn, Ga, Rb, Sr, Y, Zr, Nb, Mo, Sn, Sb, Cs, Ba, La, Ce, Nd, Sm, Gd, Dy, Er, Yb, Hf, Ta, Tl, Pb, Bi, Th, U) were assembled. This number was reduced to 22 (Na, Mg, Al, Si, K, Ca, Ti, Mn, Fe, Zn, Rb, Sr, Y, Zr, Nb, Ba, La, Ce, Nd, Pb, Th, U) based on the most frequently measured and reported elements among the published and unpublished obsidian data. For example, Cu values were reported for fewer than 7% of spreadsheet entries, while Rb measurements were reported 91% of the time. This does not necessarily mean that Cu cannot be useful for

Table 1
Index of **o**bsidan sources (listed alphabetially using this manuscript's preferred nomenclature) with their supplementary tables and manuscript sections. Common alternative terms and transliterations are listed as well, as are named geological facies most often found in the obsidian literature (both lists are non-exhaustive, especially the transliteration permutations).

Table	Section	Source name (this publication)	Other names, spellings, etc.	Named facies (e.g., deposits)
Armenia				
S1	3.1.1	Aghvorik	Ashotsk, Amasia, Eni-Ël, Kechut, Sizavet	
S2	3.1.2	Arteni – Mets Arteni		
S3	3.1.2	Arteni – Pokr Arteni 1		
S4	3.1.2	Arteni – Pokr Arteni 2		
S5	3.1.3	Bartsratumb	Bartstratumb, Bardzratumb	
S6	3.1.4	Gegham – Geghasar 1	Gechasar	
S7	3.1.4	Gegham – Spitakasar 1		
S8	3.1.4	Gegham – Spitakasar/ Geghasar 2		
S9	3.1.5	Gutansar	Gutanasar, Gutansar volcanic complex	Fontan, Alapars, Dzhraber/ Djraber
S10	3.1.6	Hatis Alpha	Atis	Akunk/Akunq
S11	3.1.6	Hatis Beta		
S12	3.1.6	Hatis Gamma		
S13	3.1.6	Hatis Delta		
S14	3.1.7	Khorapor	Chorapor, Choraphor, Khoraphor, Karnyjarich	
S15	3.1.8	Ptghni		
S16	3.1.9	Syunik – Bazenk	Syunik 1, Bazenk-1, Vazenk	
S17	3.1.9	Syunik – Satanakar 1	Syunik 2, Satanakar-1	
S18	3.1.9	Syunik – Satanakar 2	Satanakar-2	
S19	3.1.9	Syunik – Satanakar 3	Bazenk-2, Bazenk-Satanakar outliers	
S20	3.1.9	Syunik – Sevkar	Syunik 3, Mets Sevkar, Pokr Sevkar	
S21	3.1.10	Tsaghkunyats 1 – Kamakar		Arqayasar/ Arkajasar, Aïkasar
S22	3.1.10	Tsaghkunyats 2 – Ttvakar		Ttujur
S23	3.1.10	Tsaghkunyats 3 – Damlik		
Azerbaijan				
S24	3.2.1	Kelbadjar / Kechal Dağ	Merkasar, Kel'badjar, Kel'bedzhar, Kelbadzhar	
Georgia				
S25	3.3.1	Chikiani 1	Paravani, Paravani Lake, Kojun Dağ	
S26	3.3.1	Chikiani 2		
S27	3.3.1	Chikiani 3		
Russia				
S28	3.4.1	Baksan / Zayukovo	Baksan River, Baksan Valley	
Turkey				
S29	3.5.1	Bingöl A (Solhan)	Bingöl peralkaline	Orta Düz; Çavuşlar
S30	3.5.2	Bingöl B (Alatepe)	Bingöl calcalkaline	Çatak; Alatepe
S31	3.5.3	Erzincan 1		Agili Tepe
S32	3.5.3	Erzincan 2		Değirimen Tepe
S33	3.5.4	Erzurum – Tambura		Güzelyurt
S34	3.5.4	Erzurum – South Erzurum	Erzurum South	Kuşakli Dağ, Başköy
S35	3.5.4	Erzurum – West Erzurum 1	Erzurum West, Erzurum-Ömertepe	Güney Dağ, Sögütlü
S36	3.5.4	Erzurum – West Erzurum 2		
S37	3.5.5	Group 3d		
S38	3.5.6	İkizdere		Haros Dağ, Rize, Büyüksulata, etc.
S39	3.5.7	Kars – Akbaba Dağ		
S40	3.5.7	Kars – Arpaçay 1	Sarıkamış North	Akhurian 1 and 2
S41	3.5.7	Kars – Arpaçay 2		
S42	3.5.7	Kars – Digor 1		Yağlica Summit
S43	3.5.7	Kars – Digor 2		Yağlica South
S44	3.5.8	Meydan Dağ	Gügürbaba Tepe	
S45	3.5.9	Muş	Mush	Mercimekkale
S46	3.5.10	Nemrut Dağ 1		
S47	3.5.10	Nemrut Dağ 2		Sıcaksu
S48	3.5.10	Nemrut Dağ 3		Kayacık
S49	3.5.10	Nemrut Dağ 4		
S50	3.5.10	Nemrut Dağ 5		
S51	3.5.10	Nemrut Dağ 6		
S52	3.5.11	Pasinler 1		Malikom Gorge, Hasanbaba Dağ
S53	3.5.11	Pasinler 2		
S54	3.5.12	Sarıkamış 1	Sarıkamış South 1C	Hamamlı, Şehitemin
S55	3.5.12	Sarıkamış 1a	Sarıkamış South 1A	
S56	3.5.12	Sarıkamış 2	Sarıkamış South 2A and 2B	Çiplak Dağ, Mescitli
S57	3.5.13	Süphan Dağ 1	Süphan I	
S58	3.5.13	Süphan Dağ 2	Süphan II	
Volcanoes misidentified as obsidian sources				
S59	3.6.1	Mount Ararat		
S60	3.6.2	Tendürek Dağ / Bayezid	Doğubeyazıt	

obsidian sourcing under some circumstances. Instead, it simply means that Cu concentrations are so infrequently measured that consensus values cannot be determined for the obsidian sources of interest here. It should be recognized, however, that the final element list is likely skewed towards the elements best measured in obsidian using forms of X-ray spectrometry – EDXRF, WDXRF, pXRF, EMPA-WDS, etc. – due simply to the prevalence of these techniques (i.e., there are more XRF datasets than NAA ones). As needed, all measurements were converted from oxides to elements (e.g., from MnO to Mn) and/or from weight percent to parts per million (ppm) (e.g., from 0.04% to 400 ppm).

It is worth stressing that, throughout this process, no one analytical technique was favored over another or given special treatment during the data processing phase. NAA measurements, for instance, were not assumed to be more or less accurate than EDXRF measurements, LA-ICP-MS measurements were not assumed to be more or less accurate than EMPA measurements, and so on. While it is common to encounter statements in the literature that a particular analytical technique is more sensitive and/or accurate than another one, these claims tend to reflect either misunderstandings or oversimplifications about the techniques. Sensitivity refers to the minimum detection limits (i.e., how small of an element's concentration can be quantified), but no technique has a constant sensitivity across the periodic table of elements. For example, some rare earth elements (REEs) can be measured by NAA at concentrations less than 1 ppm, but Sr falls below the minimum detection limits for NAA at about 10 ppm. In contrast, pXRF and EDXRF can usually measure Sr at concentrations down to 1–2 ppm, whereas REEs necessitate higher concentrations. That is, NAA is more sensitive for certain elements, while XRF is more sensitive for other elements. Accuracy

refers to the closeness of any given measurement to the true value (which is usually unknown – or at least not precisely known – for a geological specimen), and it relies on data correction and calibration, the protocols for which can vary across facilities. Hence, it is not the case that any given analytical technique inherently yields better accuracy than any other one.

An important aspect of deriving consensus values was, for each obsidian source, calculating one table entry per combination of analytical technique and laboratory. That means, for example, all of the LA-ICP-MS data from the Université d'Orléans for Meydan Dağ obsidian have been combined into one set of elemental values, despite having been originally spread among eight different publications. This was done so that any one laboratory or research group could not skew the consensus values simply because they published more articles. Under such a scheme, the same weight is given to the measurements from laboratories that reported (1) one NAA analysis in a single publication, (2) 50 LA-ICP-MS analyses in five publications, and (3) 100 EDXRF analyses in two publications. In each instance, one laboratory using one technique would correspond to one entry in the table. The use of multiple analytical techniques within a single laboratory, of course, yields multiple entries in a table. For example, the NAA, EDXRF, and ICP-MS data from MURR were treated separately since the measurements are essentially independent, despite all being generated by members of the Archaeometry Laboratory. In addition, I kept separate any major changes in instruments, such as the replacement of MURR's ElvaX EDXRF instrument with a new Thermo Quant'X model. There are some weaknesses to this approach, namely that analytical procedures can and do change over time in laboratories, but presumably this occurs for the better. Ultimately it was decided that the benefits of this approach outweighed any potential drawbacks.

The data for each laboratory were combined using a mathematical approach that could handle both tables of only summary statistics and extended tables of individual measurements. The outcome is an approximation of the mean and the standard deviation that could be calculated if all of the individual measurements were available. First, a weighted mean for each element is calculated. That is, the mean for a set of ten analyses counts for twice as much as that for a set of five analyses. Second, the standard deviation is recalculated using the variances of the original standard deviations from the new, weighted mean. Consider, as an example, that a certain EDXRF laboratory has reported three means and standard deviations for the Rb content of Meydan Dağ obsidian in three publications: (1) 200 ± 5 ppm, n = 10; (2) 190 ± 15 ppm, n = 5; and (3) 202 ± 2 ppm, n = 20. These values can all be arithmetically combined to give the mean and standard deviation for all 35 analyses. In this case, the combined result is 199.7 ± 7.2 ppm, which can be rounded to 200 ± 7 ppm. Another example can be worked with their theoretical Zr values: (1) 280 ± 10 ppm, n = 10; (2) 240 ± 30 ppm, n = 5; and (3) 270 ± 5 ppm, n = 20. In this case, the combined result for Zr is 268.6 ± 17.4 ppm, which can be rounded to 269 ± 17 ppm. Combining analyses this way should, in theory, yield overall better accuracy for a given laboratory's values.

In the supplementary tables, the reported "n" is the number of analytical observations, which is not necessarily the number of individual specimens and/or artifacts. For example, NAA does not typically involve replicate specimens or other reanalyses, so n will tend to simply reflect the number of specimens and/or artifacts in such studies. In EDXRF, however, it is more common to analyze replicates or reorient and reanalyze a specimen or, especially, an artifact. In such cases, the number of analytical observations will be higher than (and perhaps a multiple of) the number of specimens and/or artifacts. In the case of a spot analytical technique such as EMPA or LA-ICP-MS, authors might report n as the number of artifacts and/or specimens, as the number of total analyzed spots, or as some combination. For the purposes of this database, I simply give the author-reported numbers of observations without further scrutiny, so it might be that there are differences in how observations were counted.

Outlier values (e.g., anomalies, errors) were identified using a standard interquartile range (IQR) method. In brief, the IQR is the difference between the first quartile (Q1; the 25th percentile of the data points) and the third quartile (Q3; the 75th percentile). Values less than Q1 – 1.5 × IQR and those higher than Q3 + 1.5 × IQR are considered outliers. The 1.5 × IQR threshold is equivalent to a 2.7σ threshold for a Gaussian distribution. More sophisticated methods of outlier detection were considered, including the two-sided double Grubbs test (sometimes known as a maximum normalized residual test), Cochran's C test, and the Dixon test. Ultimately these tests were not used because the numbers of observations (i.e., measurements of element concentrations) remain relatively small for most of the obsidian sources, and outliers tend to be over-identified by these tests with low numbers of observations. In addition, obsidian sources with too few observations did not have any outliers determined.

Any identified outlier values were removed from the table for a given obsidian source. I decided against either leaving outliers in the tables (but still removing them from the calculations) or marking an expunged outlier with a ">" or "<" symbol in its place. There is a multitude of reasons that could lead to an outlier value, and the vast majority of these analyses were not conducted within the framework of an interlaboratory accuracy assessment, meaning that it could be somewhat unfair to highlight the outliers from any particular laboratory. For example, outliers could be due to: laboratory and specimen handling errors, inadequate specimen preparation, irregular specimen/artifact morphology (especially in the case of XRF techniques), instrument or electronic noise, instrument operating conditions, incorrect calibration or quantification model, transcription errors, uncorrected spectral interference, actual variation within a specimen or source, etc. Additionally, I have noted (Frahm, 2019: 9) that calibrating an XRF instrument using pressed-powder standards (e.g., USGS RGM-1 obsidian) but analyzing solid specimens or artifacts can add measurement error, especially for lighter elements (i.e., Ti and lighter). Furthermore, there can be technique-specific concerns. For instance, EMPA involves microscopic spot analyses, and I measured only the glass, not any mineral inclusions (e.g., microscopic magnetite grains; see the paragraph below), of the obsidian specimens. Hence, my EMPA measurements often include lower Fe values (i.e. the glass alone) than those for a bulk technique such as XRF or NAA (i.e., glass + magnetite).

Variability in the microscopic mineral inclusions inside obsidian may, in turn, increase variability in certain elements' measurements. Magnetic characterization (Fig. 3) illustrates that such inclusions are mainly grains of magnetite ($Fe^{2+}Fe_2^{3+}O_4$) and, to a lesser extent, titanomagnetite ($Fe^{2+}(Fe^{3+},Ti)_2O_4$). Other minerals occur less frequently in obsidian but can include ilmenite ($FeTiO_3$) (Figs. 4 and 5), zircon ($ZrSiO_4$) (Fig. 5), and even monazite (a phosphate rich in Ce, La, Nd, and/or Th) (Fig. 6). These particular minerals are of special interest due to their abundance of elements commonly used in obsidian sourcing. This can not only add variation to measurements but also can lead to false groupings in otherwise homogeneous obsidian. Consider, for instance, a hypothetical obsidian source that contains infrequent monazite grains – for simplicity, Ce- and La-dominant monazite – and has been sampled for geochemical analysis. When small pieces are taken for analysis, some of them might contain just one monazite grain, whereas others contain two grains. The resulting analyses could yield two groups – one with higher Ce and La, one with lower Ce and La – that reflect difference in monazite abundance, not different volcanic sources. Thus, it is worth scrutinizing subtly different chemical groups that are based exclusively on elements common to mineral inclusions within obsidian, especially Ti and Fe. Furthermore, it need not be a cause for concern if these elements exhibit greater intra-source variability than others do.

3. Obsidian sources

Poidevin (1998) covered obsidian sources in a roughly west-to-east

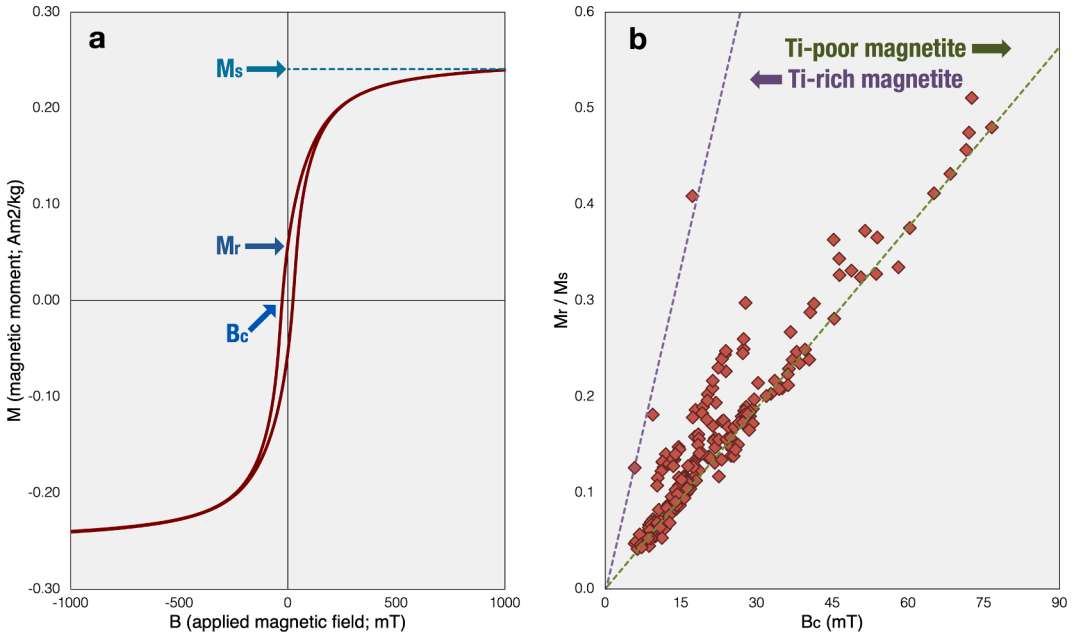

Fig. 3. Rock magnetic characterization of obsidian specimens demonstrates that their mineral inclusions are principally magnetite ($Fe^{2+}Fe_2^{3+}O_4$) and, to a lesser extent, titanomagnetite ($Fe^{2+}(Fe^{3+},Ti)_2O_4$). (a) The magnetic hysteresis loop for a magnetite-bearing specimen of Gutansar obsidian after processing (i.e., the paramagnetic contribution from the glass has been subtracted) illustrates how the saturation remanence (M_r), saturation magnetization (M_s), and coercivity (B_c) are measured. (b) Magnetic data (B_c vs. M_r/M_s) for the obsidian sources of eastern Turkey (Section 3.5) show the Ti-poor magnetite is more abundant than Ti-rich magnetite (i.e., titanomagnetite). Data collected at the Institute for Rock Magnetism, Department of Earth and Environmental Sciences, University of Minnesota-Twin Cities.

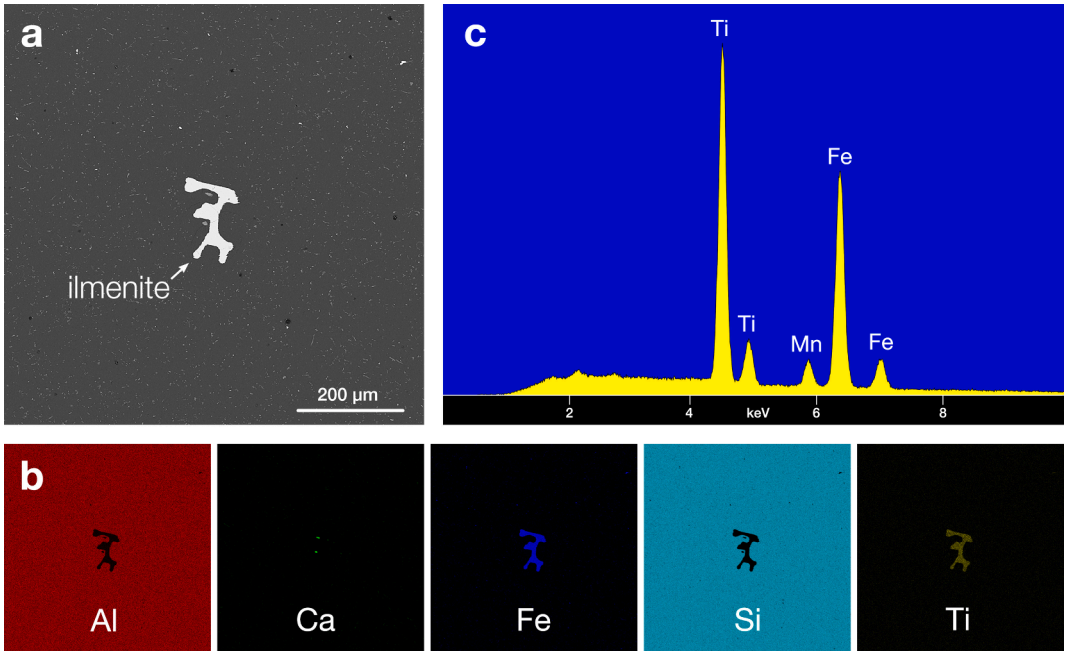

Fig 4. (a) Backscattered electron image of an ilmenite ($FeTiO_3$) inclusion (surrounded by smaller silicate and magnetite grains) in Sarıkamış 1a obsidian. (b) Element maps illustrate the distribution of Al, Ca, Fe, Si, and Ti within the same field of view, demonstrating that the mineral inclusion contains Fe and Ti. (c) An energy-dispersive X-ray spectrum for a Mn-bearing ilmenite, exhibiting the characteristic X-ray peaks for Ti, Fe, and Mn. Images collected by the author in the Electron Microprobe Laboratory, Department of Earth and Environmental Sciences, University of Minnesota-Twin Cities.

trend from Turkey's Aegean coast eastward into the Caucasus. Here, though, I follow an alphabetical order, starting with the country name and then the obsidian source name, as listed in Table 1 (which includes alternate source names). Both the sections below and the supplementary tables of elemental data follow this order. Ideally, these obsidian sources could be presented here with the same degree of detail. Unfortunately, not all of these sources are understood equally well, meaning that additional work in both the field and laboratory is still required. Table 2 summarizes the available ages for these obsidian sources, as discussed in greater detail below, and it highlights the unequal geochronological information in this region. In addition, the available geological maps vary highly in their precision and accuracy, often due to their creation

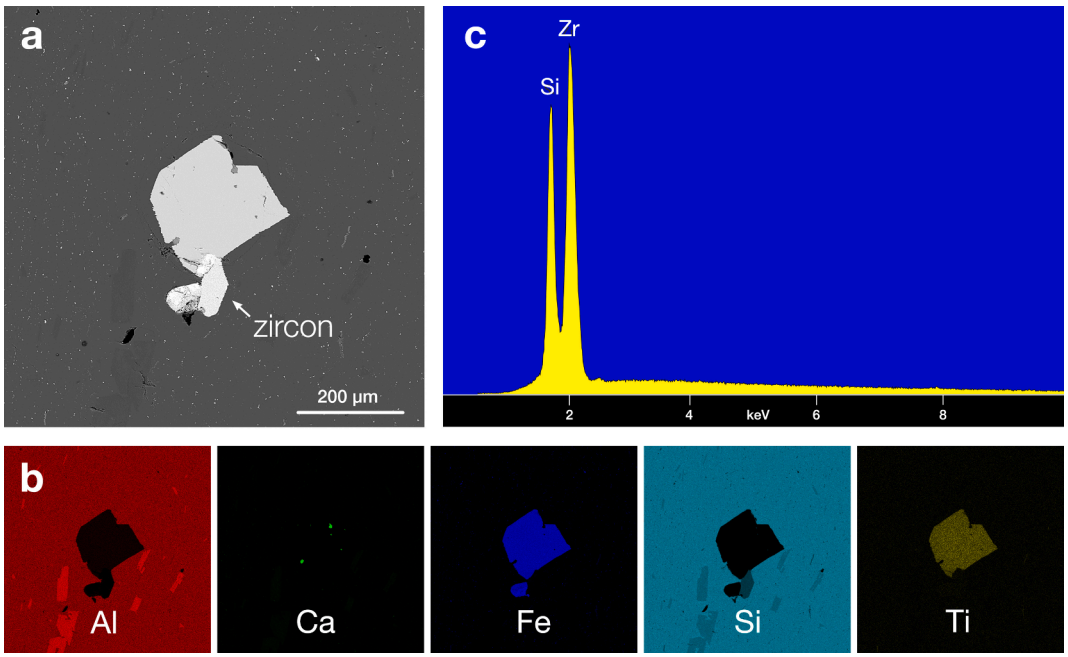

Fig 5. (a) Backscattered electron image of Kars-Arpaçay 2 obsidian with an ilmenite ($FeTiO_3$) and a zircon ($ZrSiO_4$) inclusion (surrounded by smaller silicate and magnetite grains). (b) Element maps illustrate the distribution of Al, Ca, Fe, Si, and Ti within the same field of view, demonstrating that the largest mineral inclusion contains Fe and Ti. (c) An energy-dispersive X-ray spectrum for zircon, exhibiting the X-ray peaks for Si and Zr. Images collected by the author in the Electron Microprobe Laboratory, Department of Earth and Environmental Sciences, University of Minnesota-Twin Cities.

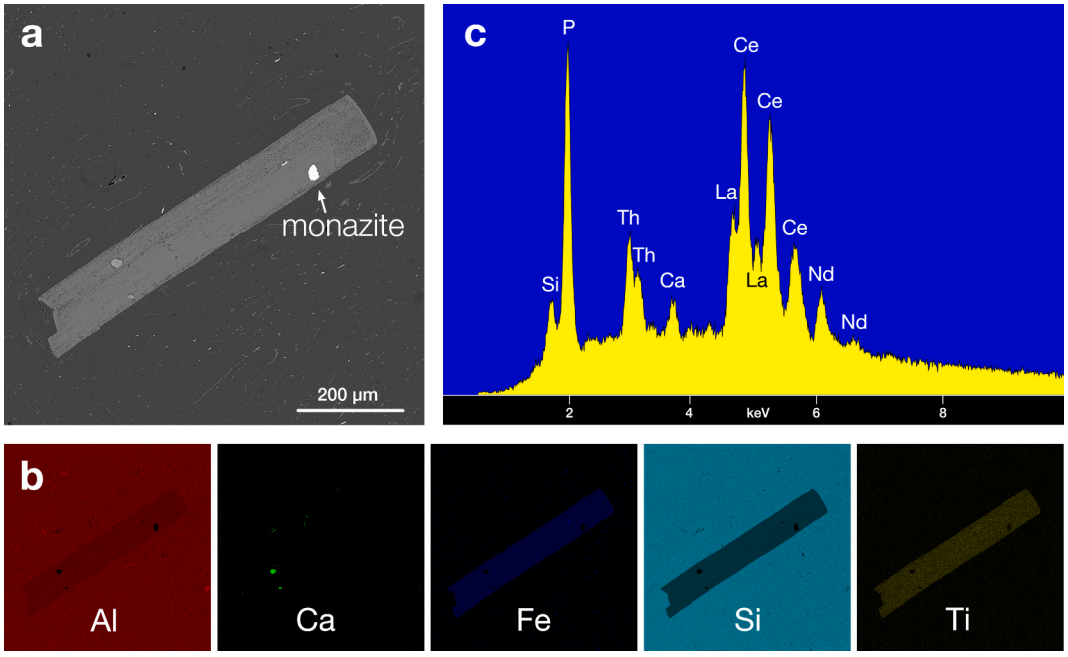

Fig 6. (a) Backscattered electron image of a feldspar crystal that contains monazite, a phosphate mineral with the formula $(Ce,La,Nd,Th)PO_4$, in Ttvakar obsidian. (b) Element maps illustrate the distribution of Al, Ca, Fe, Si, and Ti within the same field of view. (c) An energy-dispersive X-ray spectrum for a monazite, exhibiting X-ray peaks for Ce, La, Nd, and Th. Images collected by the author in the Electron Microprobe Laboratory, Department of Earth and Environmental Sciences, University of Minnesota-Twin Cities.

during the 1970s, 1960s, and earlier and their reproduction in later publications (e.g., the Arteni and Syunik complex maps in Karapetian et al., 2001 are largely redrawn from Karapetian, 1969). Furthermore, some geological maps offer conflicting interpretations (e.g., Aydar et al., 2003; Çubukçu et al., 2012 map a particular feature inside the Nerumt Dağ caldera as a slope deposit from the obsidian outcrops above, whereas Karaoğlu et al., 2005 and Özdemir et al., 2006 map it as an obsidian flow exposed in the caldera wall). Consequently, rather than reproduce maps of varying quality here, Table 3 summarizes where readers can find relevant geological maps. In the case of obsidian sources in Turkey without available geological maps, I have added scanned maps to the supplementary materials. These were the maps used in 1991 by George "Rip" Rapp (one of my graduate advisors), Tuncay Ercan (General Directorate of Mineral Research and Exploration, Turkey), and

Table 2
Summarized geochrological data for the obsidian sources in Table 1 and Section 3.

Source name	Fission-track dates	K-Ar/Ar-Ar dates
Armenia		
Aghvorik	1.0–1.1 Ma	2.3 ± 0.2 Ma
Arteni – Mets Arteni	1.2–1.4 Ma	1.45 ± 0.15 Ma
Arteni – Pokr Arteni 1	"	"
Arteni – Pokr Arteni 2	"	"
Bartsratumb	–	16.5–17.5 Ma
Gegham – Geghasar 1	0.05–0.08 Ma	0.08–0.13 Ma
Gegham – Spitakasar 1	0.12 Ma	0.20 ± 0.02 Ma
Gegham – Spitakasar/Geghasar 2	0.51 Ma??	–
Gutansar	280–320 ka	480 ± 50 ka
Hatis Alpha	330 ka	480 ± 50 ka
Hatis Beta	"	"
Hatis Gamma	"	"
Hatis Delta	"	"
Khorapor	1.5 Ma	1.75 Ma
Ptghni	–	–
Syunik – Bazenk	0.3–0.6 Ma	–
Syunik – Satanakar 1	0.4–0.6 Ma	670 ka
Syunik – Satanakar 2	"	"
Syunik – Satanakar 3	"	"
Syunik – Sevkar	0.53–0.64 Ma	0.9 Ma
Tsaghkunyats 1 – Kamakar	–	11.0 ± 0.5 Ma
Tsaghkunyats 2 – Ttvakar	–	–
Tsaghkunyats 3 – Damlik	4.2–4.6 Ma	5.4 ± 0.4 Ma
Azerbaijan		
Kelbadjar / Kechal Dağ	–	0.7 Ma
Georgia		
Chikiani 1	2.2–2.6 Ma	2.4–2.8 Ma
Chikiani 2	"	"
Chikiani 3	"	"
Russia		
Baksan / Zayukovo	2.2 ± 0.2 Ma	–
Turkey		
Bingöl A (Solhan)	4.6–5.1 Ma	4.2–4.6 Ma
Bingöl B (Alatepe)	4.3–6.0 Ma	4.4–4.7 Ma
Erzincan 1	–	0.4–0.5 Ma
Erzincan 2	–	"
Erzurum – Tambura	6.9 ± 0.3 Ma	–
Erzurum – South Erzurum	–	–
Erzurum – West Erzurum 1	–	8.4 Ma
Erzurum – West Erzurum 2	–	–
Group 3d	–	–
İkizdere	1.7–1.9 Ma	2.10 ± 0.03 Ma
Kars – Akbaba Dağ	–	–
Kars – Arpaçay 1	3.5–3.7 Ma	–
Kars – Arpaçay 2	–	–
Kars – Digor 1	2.4 ± 0.2 Ma	2.7 ± 0.3 Ma
Kars – Digor 2	"	"
Meydan Dağ	0.75–0.60 Ma	1.0–0.9 Ma
Muş	2.0–2.7 Ma	–
Nemrut Dağ 1	–	310–20 ka
Nemrut Dağ 2	–	"
Nemrut Dağ 3	–	"
Nemrut Dağ 4	–	"
Nemrut Dağ 5	–	"
Nemrut Dağ 6	–	"
Pasinler 1	5.5–6.2 Ma	5.5 ± 0.1 Ma
Pasinler 2	"	"
Sarıkamış 1	3.6–4.8 Ma	–
Sarıkamış 1a	"	–
Sarıkamış 2	"	–
Süphan Dağ 1	–	680 ± 12 ka
Süphan Dağ 2	–	"

their colleagues to collect obsidian specimens from those sources.

3.1. Armenia

The large number of obsidian sources within the modern borders of Armenia is often surprising to those unfamiliar with this highly volcanic country. Within the 65-km-long stretch between the capital Yerevan and Lake Sevan, known at the Gegham range, there are more than 120 Quaternary (Pleistocene and Holocene) volcanic centers, pyroclastic cones, and lava domes. Across all of Armenia, which is about the size of Belgium or South Carolina, that number increases to more than 500.

Table 3
Obsidian sources and their available geological maps.

Source names	References for available geological maps
Armenia	
Aghvorik	Shalaeva et al., 2019: Fig. 2; (Trifonov et al., 2017): Fig. 2
Arteni – Mets and Pokr Arteni	Frahm, 2014: Fig. 7; Karapetian et al., 2001: Fig. 5
Bartsratumb	This study: Fig. 8; Karapetian et al., 1986: Fig. 1
Gegham – Geghasar & Spitakasar	Karapetian et al. 2001: Fig. 9
Gutansar	This study: Fig. 10; Sherriff et al., 2019: Fig. 4; Karapetian et al., 2001: Fig. 3
Hatis Alpha–Delta	Frahm et al., 2021: Fig. 3; Sherriff et al., 2019: Fig. 4; Karapetian et al. 2001: Fig. 3
Khorapor	Karapetian et al. 2001: Fig. 4; Keller et al., 1996: Fig. 5
Ptghni	Sherriff et al., 2019: Fig. 5; Frahm et al., 2017: Fig. 1
Syunik – Bazenk, Satanakar, Sevkar	Karapetian et al. 2001: Fig. 11
Tsaghkunyats 1–3	Karapetian et al. 2001: Fig. 2
Azerbaijan	
Kelbadjar / Kechal Dağ	Fataliyev et al., 2022: Fig. 2; Imamverdiyev et al., 2018: Fig. 1
Georgia	
Chikiani 1–3	Biagi et al., 2017: Fig. 2; Karapetian et al., 2001: Fig. 6
Russia	
Baksan / Zayukovo	Shackley et al., 2018: Fig. 3
Turkey	
Bingöl A and B	Poidevin, 1998: Fig. 25
Erzincan 1–2	This study: Supplementary Fig. 1
Erzurum – various sources	Not currently available; see Brennan, 2000: Figs. 2 and 3
Group 3d	n/a: unknown location
İkizdere	Yeğingil et al., 2002: Fig. 1
Kars – various sources	This study: Supplementary Fig. 2
Meydan Dağ	Akköprü et al., 2019: Fig. 3
Muş	Poidevin, 1998: Fig. 25
Nemrut Dağ 1–6	Frahm, 2020: Fig. 6; Özdemir et al., 2006: Fig. 2; Karaoğlu et al., 2005: Fig. 2; etc.
Pasinler 1–2	Not currently available; see Brennan, 2000: Fig. 3
Sarıkamış 1–2	This study: Supplementary Fig. 3
Süphan Dağ 1–2	This study: Supplementary Fig. 4

3.1.1. Aghvorik

The Aghvorik obsidian source (41.08° N, 43.75° E, 1700–1800 m asl) is also known by a variety of alternative names: Ashotsk (Ashots), Amasia, Eni-Ël (Yeni-Ël), Kechut, and Sizavet (Sizevit). Situated in the southern foothills of the Djavakheti (Javakhk) range, the precise eruptive center of this obsidian remains unclear. All obsidian specimens – even those collected from outcrops several kilometers apart – exhibit a singular, homogenous composition despite their highly variable appearance. Aghvorik obsidian has been K-Ar dated to 2.3 ± 0.2 Ma (Karapetian et al., 2001), whereas Oddone et al. (2000) reported considerably younger fission-track dates of 1.0–1.1 Ma. Of these two techniques, K-Ar dating likely provides the more reliable date for Aghvorik obsidian. As a result of its age, the obsidian has low visibility due to Quaternary sedimentation, vegetation cover, and deep snow for six months of the year (Olshansky, 2018). Olshansky (2018) notes that, while high-quality obsidian can be found at this location (contrary to some accounts), such blocks tend to have relatively small diameters ca. 10–15 cm, limiting their utility for making certain types of stone tools. Table S1 summarizes the elemental data for this source.

3.1.2. Arteni: Mets Arteni & Pokr Arteni 1 and 2

The Arteni complex has two main eruptive centers (Fig. 7): Mets ("Big") Arteni (40.38° N, 43.30° E), which is the taller of the two peaks, and Pokr (or Poqr; "Small") Arteni (40.35° N, 43.78° E). The Arteni

Fig. 7. The two main eruptive centers of the Arteni complex in western Armenia – Mets ("Big") Arteni on the right side and Pokr ("Small") Arteni on the left – viewed from the Middle Palaeolithic open-air site of Barozh-12. Photograph by the author.

complex lies at the southeastern base of the Mount Aragats volcanic massif, so mentions in the literature of obsidian associated with Mount Aragats (or Aragatz) actually refer to Arteni. Satani-dar (or Satani Dar, which translates as "Satan's mountainside") is not a discrete obsidian source, as has been reported, but instead is a Palaeolithic lithic scatter on the slopes of Mets Arteni (Gasparyan et al., 2014), meaning that it likely consists of obsidian artifacts derived from a variety of sources throughout the region. Indeed, the complex is surrounded by open-air Palaeolithic sites, including Barozh-12 (Glauberman et al., 2020), and surface deflation in this semi-arid setting has created a desert pavement of artifacts, a palimpsest that, if sampled, would yield obsidian from multiple sources. Indeed, this almost certainly occurred in the "Pokr Arteni" sample of Blackman et al. (1998): out of the five tested obsidian specimens, three matched Pokr Arteni, one matched Mets Arteni, and one originated from a much farther source (Frahm, 2014). Such an outcome highlights the importance of sampling directly from geological outcrops.

Obsidian occurs as large blocks and outcrops as well as lenses and small nodules in voluminous perlite deposits, including the Aragats flow (different than Mount Aragats) that extends to the west and the Brusok quarry to the northeast. The obsidian is easily accessed from the surrounding plains, and the snow cover tends to be shallow (ca. 25 cm) and last only a few months (Badalyan et al., 2004). Fission-track dating of Arteni obsidian has yielded dates clustered ca. 1.2–1.4 Ma (Komarov et al., 1972; Wagner et al. 1976; Oddone et al., 2000; Badalian et al., 2001). In addition, a single K-Ar date for Arteni obsidian yielded an age of 1.45 ± 0.15 Ma, while a rhyolite specimen was dated to 1.60 ± 0.15 Ma (Chernyshev et al., 2006). These age ranges may well reflect the sequence of two or three obsidian-producing eruptions that led to three distinct trace-element compositions of obsidian found at the complex (e.g., Keller et al., 1996; Chataigner and Gratuze, 2014; Olshansky, 2018; Orange et al., 2021).

Table S2 summarizes the compositional data for Mets Arteni, while Table S3 and S4 list the data for Pokr Arteni 1 and 2, respectively. Thus far delineating the spatial distributions of Pokr Arteni 1 and 2 obsidian has been challenging (e.g., Chataigner and Gratuze, 2014; Olshansky, 2018) and oversimplified (e.g., Keller et al., 1996). Some researchers have assumed that the westward Aragats flow derived from Mets Arteni; however, obsidian specimens collected along the flow's southern perimeter instead exhibit a trace-elemental similarity with outcrops on the eastern slopes of Pokr Arteni (Frahm, 2014; Olshansky, 2018). The mechanism for the compositional dichotomy of Pokr Arteni 1 and 2 obsidian remains unclear, leaving two equally likely possibilities at present. First, Pokr Arteni 1 and 2 obsidian might have erupted at two different times, between which the magma slightly evolved in composition. In this scenario, Pokr Arteni 1 could have erupted second, largely breaking through and/or covering the Pokr Arteni 2 obsidian and, in turn, contributing to difficulties in its circumscription on the modern landscape. Second, like the Borax Lake obsidian source in California (Bowman et al., 1973a, 1973b), Pokr Arteni obsidian might have exhibited a continuous elemental variation in composition as it erupted, perhaps due to magma mixing, but it only occurs at the surface in two apparently discrete compositions. That is, the compositional gap between Pokr Arteni 1 and 2 might have been filled by obsidian of intermediate composition that is now buried, altered (e.g., hydrated), destroyed (e.g., remelted), or otherwise inaccessible. Further geological fieldwork at the Arteni complex would be needed to resolve this open question.

3.1.3. Bartsratumb

Bartsratumb (or Bartstratumb, Bardzratumb, etc.; Fig. 8) is included here although no artifacts, at least to my knowledge, have been matched to this little-known source of, by all accounts, poor-quality obsidian (Cherry et al., 2010; Orange et al., 2021). Karapetian et al. (1986) observe that the Bartsratumb rhyolites are aphanitic (i.e., any mineral grains are too small to be seen with the naked eye) and exhibit flow bands that range in crystallinity, varying from glassy to spherulitic. Outcrops reportedly reveal highly perlitic (i.e., hydrated, having cracks and/or spherules) obsidian poorly suited to knapping (Cherry et al., 2010; Orange et al., 2021). This is due to this obsidian's considerable age (for obsidian, at least). This lava dome has been dated by K-Ar to 16.5–17.5 Ma (Karapetian et al., 1986, 2001), making it one – even two – orders of magnitude older than other obsidian sources in Armenia. Usually obsidian does not exist for more than 10 to 20 million years before it largely degrades into perlite, and Bartsratumb obsidian falls near the upper end of this age range. In fact, Bartsratumb is even highlighted by Karapetian et al. (2001) as the oldest lava dome included in their study of rhyolitic volcanism in Armenia.

Situated along the Zangezour ridge, Bartsratumb's location (39.529° N, 45.815° E; 2450 m asl) has contributed to its lack of investigation. Specifically, it sits directly on the mountainous border between Armenia and the Nakhchivan Autonomous Republic, an exclave of Azerbaijan. Indeed, the dome lies half inside Armenia and half inside Nakhchivan, and a former border crossing, now militarized, lies less than a kilometer away. Consequently, Bartsratumb is virtually impossible to reach, survey, and sample. Hence, even those scholars who briefly mention Bartsratumb and include it on a map of obsidian sources (e.g., Blackman et al., 1998; Cherry et al., 2010) typically have not analyzed any specimens. Table S5 includes the rare measurements by Orange et al. (2021) as well as a Bartsratumb rhyolite that was measured by Karapetian et al.

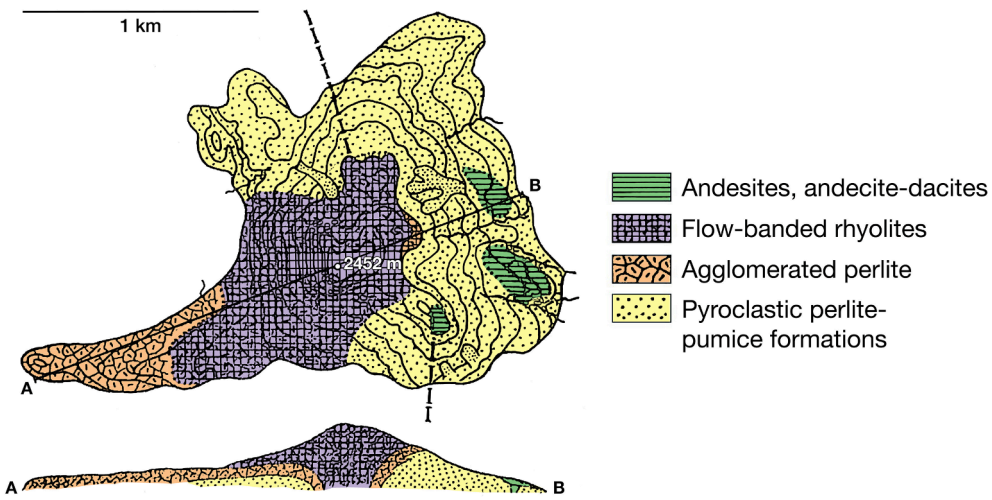

Fig. 8. Even simple geological maps for most obsidian sources in Armenia have been published in English and/or French over the years (e.g., Keller et al., 1996; Blackman et al., 1998; Poidevin, 1998; Karapetian et al., 2001). A map of Bartsratumb, though, has only appeared, to my knowledge, in a relatively obscure Russian publication almost four decades ago (Karapetian et al., 1986: Fig. 1). Hence, this figure has been redrawn, colorized, translated, relabeled, and clarified from that original map. The dashed line indicates the border between Armenia and the Nakhchivan Autonomous Republic.

(2001) by WDXRF in Armenia's Institute of Geological Sciences.

3.1.4. Gegham: Geghasar 1, Spitakasar 1, and Spitakasar/Geghasar 2

The Geghasar ("Beautiful Mountain" in Armenian; 40.11° N, 44.98° E) and Spitakasar ("White Mountain," 40.17° N, 45.01° E) eruptive centers sit high in the Gegham (or Geghama) mountain range at ca. 3000 and 3300 m asl, respectively, only 5 km apart. Fig. 9 shows how Spitakasar stands out from and is readily accessed from the surrounding mountain steppe grasslands, which are seasonally inhabited by herders during the summer months. Snow cover can last eight months of the year and be ca. 2 m deep (Badalyan et al., 2004), and such a remote location has complicated study efforts. Blackman et al. (1998), for example, list Spitakasar as one of their few uncharacterized obsidian sources.

Geghasar 1 (Table S6) and Spitakasar 1 (Table S7) obsidian have very similar (Olshansky, 2018) but not identical, as is sometimes claimed (Keller et al., 1996; Chataigner and Gratuze, 2014), trace-element compositions. It seems likely, though, that non-destructively differentiating artifacts from these sources will be impractical in many instances due increased error associated with irregular surface morphology, weathering and hydration, small size, etc. Nevertheless, their compositional data are reported separately here. Their elemental affinity of Spitakasar 1 and Geghasar 1 obsidian is likely due to their eruption from a shared magma chamber, which experienced relatively little geochemical evolution between these two volcanic events. Dating has established that Spitakasar 1 obsidian is the older of the two. Badalian et al. (2001) found a fission-track age of 0.12 Ma for a Spitakasar obsidian specimen and ca. 0.05–0.08 Ma for five Geghasar specimens, making these two obsidian sources considerably younger than others found in Armenia. Lebedev et al. (2013) report slightly older K-Ar ages: 0.20 ± 0.02 Ma for one Spitakasar obsidian specimen and ca. 0.08–0.13 Ma for three Geghasar obsidian and rhyolite specimens. As noted for other Armenian obsidian sources (see, for example, Gutansar in Section 3.1.5), the fission-track dates appear to be underestimates but systematically so. Importantly, as little as 40–50 ka between these two eruptions is consistent with such small differences in their trace-element values. Another difference between the two is appearance. Spitakasar 1 obsidian specimens typically contain white phenocrysts, most likely high-temperature alkali (potassium) feldspars such as sanidine, visible to the naked eye (Badalyan et al., 2004; Chataigner and Gratuze, 2014; see also photos in Olshansky, 2018: Fig. 5.11).

The obsidian that, for lack of a better name, I have here termed "Spitakasar/Geghasar 2" (Table S8) is enigmatic. It was collected by my colleagues, Armenian volcanologists Khachatur Meliksetian and the late Sergey Karapetian (both of the Institute of Geological Sciences, National Academy of Sciences), near the western base of the Spitakasar lava dome as approached from between two nearby pyroclastic cones, Vishapasar

Fig. 9. Approaching the Spitakasar obsidian source (left background) from the west on the surrounding mountain steppe in mid-summer, when the Gegham mountains are inhabited by small encampments of herders (right foreground). During wintertime, snow can be 2-m deep here. Photograph by the author.

and Nazeli. Spitakasar/Geghasar 2 obsidian stands out in composition to Spitakasar 1 and Geghasar 1 obsidian, and such a considerable difference raises the possibility of an earlier period of rhyolitic volcanism in the vicinity. Indeed, Lebedev et al. (2013) list Spitakasar 1 obsidian as a product of Phase III volcanism in the Gegham highlands and Geghasar 1 obsidian as a product of Phase IV volcanism. In addition, Karapetian et al. (2001) propose that there had been at least four or five eruption episodes at Spitakasar based on their mapping of the lava flows. Spitakasar/Geghasar 2 obsidian neither matches any other known volcanic source nor any of the "unknown" obsidian artifacts in the literature, so we do not believe that it was accidently sampled from an anthropogenic context. Interestingly, Karapetian et al. (2001) report a markedly older fission-track date for a specimen of Spitakasar obsidian: 0.51 Ma, which would make it consistent with Phase II (ca. 0.58–0.47 Ma) volcanism of Lebedev et al. (2013). It would be difficult to reconcile such different fission-track ages – 0.12 vs. 0.51 Ma – for the same obsidian source, and it is tempting to ascribe the 0.51-Ma date to Spitakasar/Geghasar 2 obsidian, rather than Spitakasar 1 obsidian. Another clue may lie in the relatively high Ba concentration of Spitakasar/Geghasar 2 obsidian (a mean of 360 ppm) compared to Spitakasar 1 (27 ppm) and Geghasar 1 (18 ppm) obsidian. Ba tends to be removed from rhyolitic magma during the formation of feldspar crystals, which can remain inside the magma chamber (e.g., crystal sinking), leaving the resulting obsidian with Ba diminished levels. The likely feldspar phenocrysts visible in Spitakasar 1 obsidian appear consistent with such a mechanism of magma changing from high to low Ba levels over the span of hundreds of millennia (Anderson et al., 2000). It is also highly important to note that I have identified five Spitakasar/Geghasar 2 obsidian artifacts at three Palaeolithic sites in Armenia: two from the Middle Palaeolithic open-air site of Barozh-12 (Glauberman et al., 2016, 2020); two from the Middle Palaeolithic rockshelter site of Lusakert Cave 1 (Adler et al., 2012; Gasparyan et al., 2014; Frahm et al., 2016); and one from the Upper Palaeolithic cave site of Aghitu-3 (Kandel et al., 2011, 2017; Frahm et al., 2019). Perhaps significantly, Barozh-12 and Aghitu-3 are almost equidistant (110–120 km linearly) from Spitakasar but in nearly opposite directions.

It is also worth addressing concerns found in the literature (Badalyan et al., 2004; Chataigner and Gratuze, 2014) regarding the potential for a tributary of the Azat River, which flows past the base of the Geghasar outcrops, to transport obsidian downstream to much lower elevations, perhaps even as far as the Ararat Depression. For example, when discussing Geghasar, Badalyan et al. (2004) mention that small obsidian clasts occur downstream near the village of Garni. To address this issue, I conducted surveys of (1) alluvial terraces along the Azat River between the villages of Geghard (ca. 1700 m asl) and Garni (ca. 1200 m asl), a drop in 500 m over a linear distance of 9 km, and (2) small streams in the highland steppe between the outcrops and Geghard. Indeed, obsidian pebbles with maximum dimensions up to 4 cm (or occasionally more) were found along the river bed and in the profile of an alluvial terrace. It would have been simple to conclude that the pebbles represent secondary deposits of Geghasar obsidian; however, pXRF analyses revealed that this would be incorrect: all of the obsidian pebbles were, instead, Gutansar obsidian. In fact, obsidian found in and along the river and stream beds reflects a modern contamination of the landscape by degraded concrete, which, throughout much of Armenia, contains Gutansar obsidian pebbles and fragments. Concrete production, still today, uses Gutansar pumice/perlite deposits in direct contact with obsidian layers and dikes. Similarly, a number of potential "pumice" clasts (up to 10 cm in maximum dimension), all containing visible subcentimeter obsidian fragments, instead turned out to be tumbled, rounded concrete. Indeed, abundant obsidian-bearing concrete was found in various stages of degradation all along the built environment of the Azat River. Consequently, descriptions of secondary obsidian deposits must, in such an environment, take into account this cause of modern contamination, and any obsidian pebbles or fragments discovered on the surface, in river beds, etc. must be assumed to reflect contamination from obsidian-bearing concrete until proven otherwise.

3.1.5. Gutansar

The Gutansar (or Gutanasar) volcanic complex (40.37° N, 44.68° E) consists of a pyroclastic cone and eruptive center, two named lava domes (Fontan/Fantan and Alapars/Alaphars) to the north, and a variety of named obsidian exposures (e.g., Avazan, Djraber, Gyumush, Nurnus) around the complex. It is also sometimes known as the "Hrazdan structure" due to its location along the river of the same name or the "Djraber extrusion" due to a mining-related exposure near a village of the same name. Obsidian from all of these locations is geochemically indistinguishable and was produced during either a single eruptive event or a series of closely timed ones (Frahm et al., 2014). It is too simplistic to refer to this immense extrusive body as the Gutansar obsidian "flow," but there is no clear term to describe such a voluminous eruptive feature with both extrusive and near-surface debris-flow aspects. An important aspect of this is a long-standing geographic bias in the relevant geological research. Descriptions and models of rhyolitic volcanism are principally based on the tectonically simple cases found in the Pacific Northwest of North America (e.g., Fink, 1980, 1987; Eichelberger et al., 1986; Fink and Manley, 1987). For example, spanning from California to British Columbia, obsidian sources in the Cascade volcanic arc are the products of the oceanic Juan de Fuca plate subducting under the continental North American plate. Armenian geologists have long noted, though, that such simple models do not accurately describe volcanism in the Caucasus (Shirinian and Karapetian, 1964), where the Arabian, Eurasian, Anatolian, and African plates interact in complex ways and yield different magmatic conditions. Specifically, Shirinian and Karapetian (1964: 26) report that, in comparison to rhyolitic lava domes that occur elsewhere in the world, such "volcanoes of Armenia are represented by fan-like, stratified, and more complicated forms.".

Recent remapping of the Gutansar complex by the Palaeolithic Archaeology, Geochronology, and Environments of the Southern Caucasus (PAGES) Project (of which I was a team member) expanded and refined the spatial distribution of the obsidian-bearing lava (see Sherriff et al., 2019). This map (Fig. 10) shows why Gutansar obsidian, even when sampled from exposures nearly 13 km apart, is geochemically indistinguishable (Frahm et al., 2014): despite the various names, these exposures are all aspects of the same volcanic feature. Unlike past interpretations, it now appears that Fontan and perhaps also Alapars are not separate dome-shaped, obsidian-producing rhyolitic extrusions related to, maybe along a shared fault line with, the main Gutansar eruptive center and flow. Instead, my colleagues and I have proposed that Fontan, at least, is a subsequent crypto-dome that created a "blister" beneath the obsidian-bearing flow, giving it the appearance of a typical lava dome (Malinsky-Buller et al., 2021). The data in Table S9 combine measurements from all of the named facies at the Gutansar complex.

The exact age of Gutansar obsidian is somewhat unclear. The most recent fission-track dates all cluster ca. 310 ± 30 ka: and 310 ± 30 and 320 ± 30 ka for Gutansar, 280 ± 30 and 310 ± 20 ka for Alapars, and 300 ± 20 and 320 ± 20 ka for Fontan (Badalian et al., 2001). These ranges are consistent with older fission-track dates (Komarov et al., 1972; Wagner et al., 1976; Wagner and Weiner, 1987) and attest to contemporaneous, or nearly so, emplacement across the complex. Unfortunately, these dates appear to be underestimates for some unknown reason. Consider that artifacts made from Gutansar obsidian have been identified at the nearby Lower Palaeolithic site of Nor Geghi-1 along the Hrazdan River (Adler et al., 2014; Frahm et al., 2020). The upper artifact layer at the site has been well-dated to 335–325 ka (Adler et al., 2014), and its lower layer has been provisionally dated to ca. 425–375 ka (Frahm et al., 2020). It, of course, cannot be that artifacts at Nor Geghi-1 predate the Gutansar eruption. Lebedev et al. (2013) has, more recently, reported K-Ar ages for two obsidian specimens from this complex: 480 ± 50 ka and 1.2 ± 0.5 Ma. Given the uncertainty of the latter date (i.e., half a million years), the former – 480 ± 50 ka – is a more reasonable

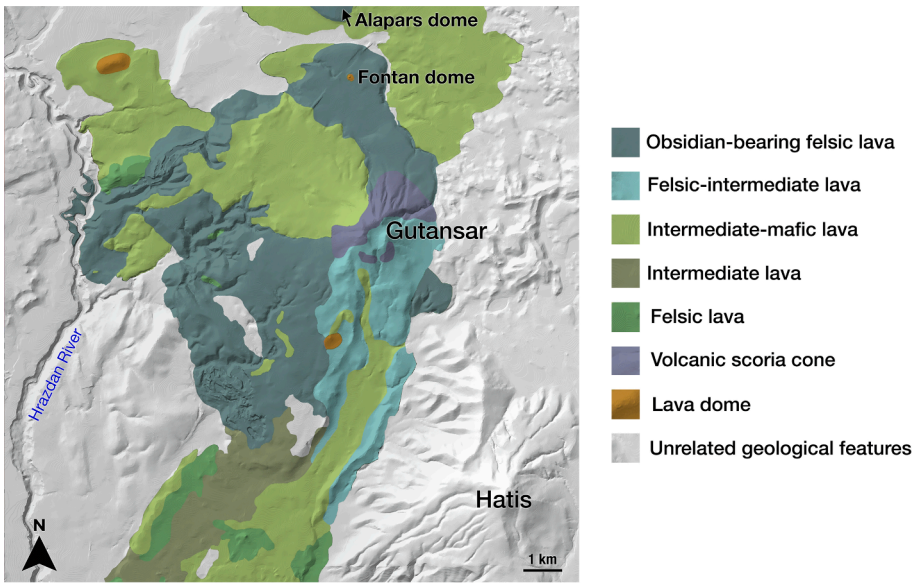

Fig. 10. The updated geological map of the Gutansar complex, remapped by the Palaeolithic Archaeology, Geochronology, and Environments of the Southern Caucasus (PAGES) Project, refines the distribution of the obsidian-bearing lava around this volcano (Sherriff et al., 2019).

estimate for the true age of Gutansar obsidian, and it is consistent with the 1970 s-era K-Ar date of ca. 550 ka for Gutansar obsidian reported by Komarov et al. (1972).

3.1.6. *Hatis Alpha, Beta, Gamma, and Delta*

Hatis (or Atis) volcano (40.30° N, 44.72° E) lies just to the southeast of Gutansar. This volcano is, to my knowledge, unique in the world in that it exhibits elemental "steps" in obsidian composition with elevation, as my colleagues and I have documented in-depth (Frahm et al., 2021). Prior studies identified only one or two obsidian compositions at Hatis (e.g., Hatis A and B in Keller et al., 1996; one in Blackman et al., 1998; Hatis 1 and 2 in Chataigner and Gratuze, 2014). Conducting pXRF analyses in the field at 80 loci across the volcano revealed four distinct compositions of obsidian (Fig. 11a) with well-defined spatial distributions, corresponding to four sources following the definition in Section 2. Each chemical type of obsidian occurs over a range of elevations: Alpha obsidian is the lowest at ca. 1590–1700 m asl, Beta at ca. 1560–1830 m asl, Gamma at ca. 1710–1910 m asl, and Delta obsidian is the highest at ca. 1960–2100 m asl. Our surveys also recognized dark grey, aphanitic, obsidian-like trachytes (such as that reported in Frahm, 2019 with outcrops near 40.27° N, 44.73° E), which would be excellent lithic material and might receive a field description such as dacite or rhyolite. The compositions of Hatis Alpha, Beta, Gamma, and Delta obsidian are summarized in Table S10, S11, S12, and S13, respectively.

The troubled history of the Hatis chronology is also detailed by Frahm et al. (2021). Similar to the discrepancies for Gutansar obsidian, fission-track dating produced an age of ca. 330 ka while K-Ar dating of the same material yielded an age of ca. 650 ka (Komarov et al., 1972). Subsequent K-Ar dates had, in some cases, large uncertainties (e.g., 740 ± 250 ka) but generally suggest an age of roughly half a million years (480 ± 50 ka) for Hatis obsidian (Lebedev et al., 2013). It seems fair to conclude that Gutansar and Hatis obsidian are products of the same period of volcanic activity within the region.

Two possible models to explain the compositional variation of Hatis obsidian are also detailed by Frahm et al. (2021), and these models are illustrated here in Fig. 11b–c. The first possibility, as shown in Fig. 11b,

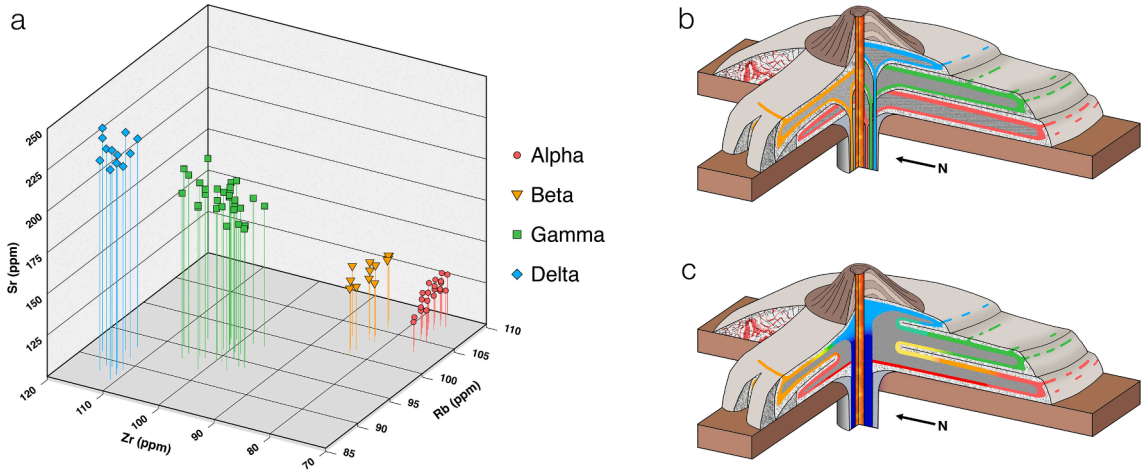

Fig. 11. Four distinct compositions of obsidian occur at Hatis volcano. (a) A three-dimensional elemental scatterplot of Rb, Sr, and Zr illustrates the four obsidian compositions among geological specimens from Hatis. Frahm et al. (2021) propose two mechanisms for this trend in obsidian composition: (b) the four types reflect a series of closely timed eruptions, yielding four similar but still distinct lavas stacked atop one other, or (c) the magma chamber was chemically zoned such that the lava changed in composition as it erupted but folded over onto itself, producing four discrete geochemical steps rather than continuous variation at the surface. Illustrations from Frahm et al. (2021).

is that the four obsidian types reflect a sequence of closely timed eruptions between which the magma slightly evolved in composition, yielding four chemically similar but still somewhat distinct lavas which are stacked one on top of the other. The other possibility, as shown in Fig. 11b, is that the magma chamber was geochemically zoned such that, over the course of a single eruption, the lava continuously changed in trace-element composition. In this scenario, the viscous lava folded over onto itself, yielding what appears to be four discrete elemental steps, rather than continuous chemical variation, exposed at or near the surface. It should also be mentioned that all four chemical types of Hatis obsidian have been identified at the Lower Palaeolithic open-air site of Nor Geghi 1 (Frahm et al., 2021).

3.1.7. Khorapor

Khorapor (Chorapor, Choraphor, Khoraphor, etc.; sometimes called Karnyjarich or Karnyjarykh in older publications) volcano lies just to the south of Lake Sevan in the Vardenis mountain range (40.053° N, 45.629° E, 2900 m asl). A K-Ar date produced an age of ca. 1.75 Ma (Karapetian et al., 2001), whereas fission-track dating resulted in an age of ca. 1.5 Ma (Badalian et al., 2001). Keller et al. (1996: 72) describe the obsidian as occurring "in the form of individual lenses and brecciated part of the major rhyolitic flow" of the volcano, consistent with the low obsidian abundance and quality (i.e., small nodules with mineral inclusions visible to the naked eye) noted by Badalyan et al. (2004) and, in turn, its low desirability as an exploitable obsidian resource. Badalyan et al. (2004) also note that the volcano is covered with more than a meter of snow for half of the year, making it accessible only during summer, and no obsidian quarries, workspaces, or even artifacts have been found on its slopes. Indeed, Khorapor obsidian appears to have hardly, if at all, been used in the past. To my knowledge, the only Khorapor obsidian recovered from any archaeological context is a small, unknapped pebble inside a ceramic sherd from the Chalcolithic site of Mentesh Tepe (Palumbi et al., 2018). Table S14 summarizes the chemical data for Khorapor obsidian. A sister volcano of Khorapor, called Sandukhkasar, is occasionally mentioned as having obsidian, but Keller et al. (1996: 72) report only "dense glass-rich rhyolite, not real obsidian" there.

3.1.8. Ptghni

Ptghni obsidian is included here for the sake of completeness, given that it is only known from pebble-/cobble-sized clasts in an alluvial-lacustrine deposit along the Hrazdan River and that, so far, no artifacts have been attributed to it. This obsidian was discovered by me and my colleagues in 2016 ca. 2 km to the southwest of the village of Ptghni, and we have documented its geological context (40.252° N, 44.564° E) in detail elsewhere (Frahm et al., 2017). It was deposited there after having eroded out of an upstream origin, and the sediments were later covered by mafic lavas and then exposed by downcutting of the Hrazdan River due to tectonic uplift of the region. At least five lavas and two alluvial-lacustrine sedimentary sequences are exposed above Upper Miocene (ca. 12–5 Ma) marine deposits at this location within the Hrazdan Gorge. Based on the stratigraphy, these lavas and, in turn, the sediments sandwiched between them predate ca. 441 ka (Adler et al., 2014). The obsidian clasts found at this exposure are too small to be well suited for tool production; however, the primary source (i.e., the original flow or dome) and/or other secondary deposits might have larger blocks and clasts. The primary Ptghni obsidian source likely lies somewhere within the Hrazdan River basin, and it must have been exposed, at least partially, sometime during the past to allow for erosion and transport of the clasts. It is unknown in what form the source still exists, if at all. The red-brown colors of some clasts necessitate the conversion of microscopic black magnetite crystals (Fe_3O_4) to hematite (Fe_2O_3) and, in turn, exposure to oxygen while still hot. Thus these clasts might have derived from surface protrusions of obsidian rather than the deeply buried basal zone of the flow (Hughes and Smith, 1993). That is, these small obsidian clasts may have eroded from any surface outcrops and been fluvially reworked and transported, whereas other parts of the obsidian flow could have stayed buried and/or been reburied by sedimentation and lava flows. Table S15 summarizes my data for Ptghni obsidian, which has yet to be analyzed in other laboratories.

3.1.9. Syunik: Bazenk, Satanakar 1–3, and Sevkar

The Syunik (alternatively transliterated as Sjunik) obsidian sources (sometimes termed the Sisian or Vorotan Group) lie within the Syunik Province of southeastern Armenia and within the Vorotan River basin. The Syunik sources have been most intensively surveyed by Cherry et al. (2010), who analyzed 68 geological source specimens. Unfortunately, these sources, in particular Satanakar, lie along or near the contested border between Armenia and Azerbaijan, and since the 2006–2007 fieldwork of Cherry et al. (2010), follow-up research has become increasingly difficult to conduct safely.

Bazenk (or Vazenk) (39.77° N, 45.86° E) is the highest (ca. 3200 m asl) of the Syunik sources, and as a result, it is snow-covered, with depths greater than 1 m, for the longest fraction of the year. Cherry et al. (2010) also describe its obsidian as opaque with a grainy texture, which makes it less attractive for knapping in comparison to the smoother, translucent obsidian from the other Syunik sources. Table S16 summarizes the elemental values for Bazenk obsidian. Obsidian specimens from Bazenk have only been fission-track dated, yielding ages of 0.3–0.6 Ma (Badalian et al., 2001; Karapetian et al., 2001).

Cherry et al. (2010) also report a "Bazenk-2" obsidian that they sometimes instead label "Bazenk-Satanakar outliers." The volcanic origin of "Bazenk-2" obsidian remained unclear to them. Geochemically the source specimens appeared to match outliers from Satanakar volcano and exhibited a much greater chemical affinity to Satanakar obsidian than to their Bazenk-1 obsidian (which is simply Bazenk obsidian here). Furthermore, the three "Bazenk-2" specimens did not cluster together on the landscape and were scattered amongst the other twelve "geological hand-samples" that they collected in the vicinity. Cherry et al. (2010:157) ultimately conclude that the "Bazenk-2" source is likely unrelated to Bazenk-1, despite the choice of name. It is noteworthy that the "Bazenk-2" specimens exhibit an even lower suitability for knapping: "Bazenk-2 samples have abundant white phenocrysts, appear more gray in color, and have a coarser texture" (Cherry et al., 2010: 156). What Cherry et al. (2010) describe, in my view, is consistent with the transport of a low-quality lithic raw-material to a better raw-material source and, subsequently, the discard of the lesser material in favor of collecting better toolstone. As detailed below, the Bazenk-2 obsidian of Cherry et al. (2010) is, instead, considered here to be Satanakar 3.

Satanakar (39.79° N, 45.82° E, ca. 2960 m asl) obsidian has been fission-track dated, yielding an age range of 0.4–0.6 Ma (Badalian et al., 2001; Karapetian et al. 2001), and was recently Ar-Ar dated to ca. 670 ka (Sugden et al., 2021). Badalyan et al. (2004) refer to three closely spaced volcanic peaks and domes as obsidian sources called Mets ("Big") Satanakar, Michnek ("Intermediate") Satanakar, and Pokr ("Small") Satanakar, despite having no obsidian specimens from the latter two. Of the three, only Mets Satanakar appears to have produced obsidian, at least of sufficient quality and quantity to be useful as a resource in the past. For example, the geological map of Kaparetian et al. (2001) indicates only pumice, perlite, and rhyolites at Pokr Satanakar – no obsidian deposits were mapped there. Cherry et al. (2010), too, only located obsidian at Mets Satanakar, not Michnek or Pokr Satanakar.

Cherry et al. (2010) identified two similar but still distinct compositions of Satanakar obsidian in addition to, as discussed above, Satanakar outliers seemingly the same as their "Bazenk-2" obsidian. The groups were best distinguished, according to Cherry et al. (2010), with a scatterplot of La vs. Ce (digitized and reproduced here as Fig. 12a). Unfortunately, Cherry et al. (2010) published only summary statistics for their reported chemical groups, and just two scatterplots (La vs. Ce and La vs. Th) contain extractable elemental values for each analyzed obsidian specimen. Hence, the ability to make direct comparisons to other data sets is limited; however, I maintain that there is sufficient

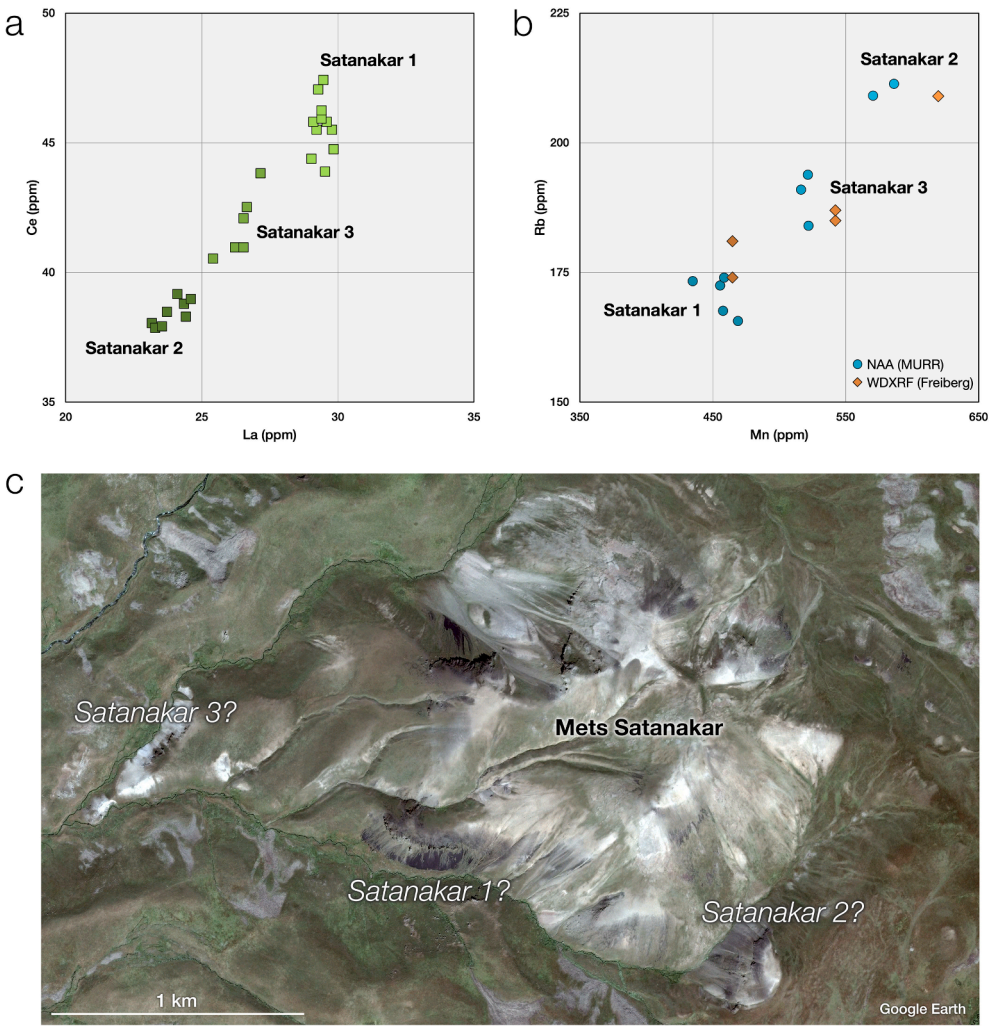

Fig 12. Proposed three compositions of Satanakar obsidian. (a) The scatterplot of La vs. Ce from Cherry et al. (2010: Fig. 5) has been digitized (using WebPlotDigitizer v 4.6 to extract the values) and color-coded in order to highlight the proposed three compositions in their NAA data. (b) Independent WDXRF (Keller et al., 1996) and NAA (Frahm et al., 2016) data also exhibit three clusters in a Mn vs. Rb scatterplot for the analyzed Satanakar obsidian specimens. (c) Provisional placement of the three obsidian compositions on the Mets Satanakar landscape. The Google Earth image is reproduced here in accordance with Google's Terms of Service and General Guidelines regarding fair use in publications (©2023, Maxar Technologies, Landsat / Copernicus Imagery collected on 11 August 2016).

evidence to support not only their Satanakar 1 and 2 as distinct obsidian compositions but also the "outliers" as their own elemental cluster that I label "Satanakar 3" (in place of their "Bazenk-2"). Fig. 12b shows that a Mn vs. Rb scatterplot with both WDXRF data from the University of Freiberg (Keller et al., 1996) and NAA data from MURR (Frahm et al., 2016) exhibits three clusters, not two, of Satanakar obsidian specimens. The appearance of these three clusters in data from two independent analytical techniques, laboratories, and collections supports their interpretation as "real" elemental clusters rather than, say, a reflection of interlaboratory variation or some measurement error. Furthermore, these three clusters can be – provisionally, at least – placed on the landscape (Fig. 12c). Cherry et al. (2010) point out that Satanakar 1 corresponds to the immense obsidian exposure on the southern face of Mets Satanakar, whereas Satanakar 2 seems associated with the southeastern outcrops. Furthermore, based on the available field notes, Satanakar 3 obsidian seems to derive from obsidian outcrops or deposits on the western slopes. I considered another nomenclature for Satanakar 1, 2, and 3 – Satanakar South, East, and West, respectively – but decided that such spatial circumscription is still too provisional. It should also be emphasized that these are subtle trace-element differences, and Satanakar 1–3 may not be readily distinguishable among artifacts, in practice, especially for non-destructive analyses of small, weathered, and/or irregularly shaped artifacts (in comparison to specimens that are freshly fractured or polished, flat, and smooth). Table S17, S18, and S19 summarize, as conceptualized here, the data for Satanakar 1, 2, and 3 obsidian, respectively.

Sevkar (39.82° N, 45.82° E, ca. 2700 m asl) is the lowest of the Syunik sources, and its obsidian is spread across the largest surface area. Sevkar obsidian has been fission-track dated to ca. 0.53–0.64 Ma and K-Ar dated to ca. 0.9 Ma (Komarov et al., 1972; Karapetian et al., 2001; Badalian et al., 2001), which is roughly contemporaneous with Bazenk and Satanakar obsidian. Varied publications refer to two Sevkar obsidian sources: Mets ("Big") Sevkar and Pokr ("Small") Sevkar ca. 2 km to the southwest. Cherry et al. (2010) established that the Sevkar obsidian deposits are chemically indistinguishable and, consequently, corroborated speculation (Badalyan et al., 2004) and geological maps (Karapetian et al., 2001) that Mets and Pokr Sevkar obsidian outcrops are both aspects of one large flow that has been partially obscured by later basalt flows. Chataigner and Gratuze (2014) also found a single composition of Sevkar obsidian and combined the measured Mets and Pokr Sevkar specimens into their "Syunik 3" composition. Table S20 summarizes the interlaboratory data and consensus values for Sevkar obsidian.

It should be kept in mind that Syunik gullies, streams, and rivers have alluvially transported (and rounded) obsidian from these sources, sometimes mixing them. For example, field surveys between the Vorotan River and the Sevkar and Satanakar obsidian sources, conducted in 2013 by my colleagues in the Tübingen-Armenian Paleolithic Project, identified streams and gullies containing rounded obsidian clasts, which I determined to be a mixture of Sevkar and Satanakar obsidian using pXRF.

3.1.10. Tsaghkunyats 1–3: Kamakar, Ttvakar (Ttujur), and Damlik

The Tsaghkunyats (alternatively transliterated as Tsakhkunjats,

Tsaghkunjats, Tsaghkuniats, etc. or sometimes called the Damlik volcanic complex) obsidian sources do not appear on the source map of Keller et al. (1996) or in the database of Poidevin (1998). The three obsidian sources (all ca. 2000–2800 m asl) in the Tsaghkunyats mountains, following my nomenclature (e.g., Adler et al., 2014), are: Kamakar (Tsaghkunyats 1; ca. 40.62° N, 44.42° E), Ttvakar (or Ttujur; Tsaghkunyats 2; ca. 40.59° N, 44.47° E), and Damlik (Tsaghkunyats 3; ca. 40.65° N, 44.38° E). Chataigner and Gratuze (2014) and those scholars who cite them (e.g., Orange et al., 2021) refer to two, not three, Tsaghkunyats obsidian sources. This appears to reflect an overreliance on Ba and Zr to define sources, presumably because that is how Renfrew and colleagues (e.g., Cann and Renfrew, 1964: Fig. 2; Renfrew et al., 1965: Fig. 4; Renfrew et al., 1966: Fig. 2) did so. Specifically, Chataigner and Gratuze (2014: 33) state that "Tsaghkunyats obsidian forms two well-identified compositional groups" in their Ba vs. Zr plot, which I have digitized from their figure (because only summary statistics were published) and recreated here as Fig. 13a. Oddly, their own Nb/Zr vs. Y/Zr scatterplot (digitized and reproduced as Fig. 13b), clearly exhibits three distinct trace-element groups, each corresponding to an individual obsidian source: Kamakar, Ttvakar, and Damlik. Yet Chataigner and Gratuze (2014: 33) hold that this plot shows "two groups," and they combine Damlik and Ttvakar into a single group. Their reasoning might have derived from Badalyan et al. (2004: 449), who wrote that NAA has "identified two separate groups, originating respectively from the Damlik and Ttvakar volcanoes… on the one hand, and the Kamakar source, on the other" and list Blackman et al. (1998) as the citation for this statement. Blackman et al. (1998), however, analyzed only two of the three Tsaghkunyats sources – Damlik and Kamakar – and noted that Ttvakar had not been sampled for the study. Table S21, S22, and S23 summarize the data for Kamakar, Ttvakar, and Damlik obsidian, respectively.

The Tsaghkunyats sources are among the oldest in Armenia, and the available geochronological data suggest that the obsidian formed during at least two different volcanic phases. Damlik obsidian has been fission-track dated, yielding ages of ca. 4.2–4.6 Ma (Oddone et al., 2000; Badalian et al., 2001), and it has a corresponding K-Ar date of 5.4 ± 0.4 Ma (Karapetian et al., 2001). Consequently, Karapetian et al. (2001) assign its eruption to a volcanic phase ca. 4.5–7.5 Ma. In contrast, with its K-Ar date of 11.0 ± 0.5 Ma, Karapetian et al. (2001) attribute Kamakar obsidian to an even earlier volcanic phase ca. 10–17 Ma. Ttvakar obsidian has apparently not been dated thus far, but it would be interesting to know if it falls chronologically, not just compositionally, between Kamakar and Damlik obsidian.

It should be kept in mind that, given the age and elevation of the Tsaghkunyats sources, alluvial and colluvial secondary deposits are found in and around these mountains, some of which contain clasts and blocks of obsidian from multiple sources. The named Hankavan deposit, near the headwaters of the Marmarik River, is one such example, and it seems to draw obsidian primarily from Damlik but also, to a lesser extent, Ttvakar. The two principal rivers able to transport small obsidian pebbles away from these mountains are the Marmarik, which flows to the east toward Lake Sevan, and the Kasakh, which flows to the south toward the Ararat Depression. In fact, my colleagues located a fluvial channel deposit (40.16° N, 44.39° E, 900 m asl) in the Ararat Depression that contained millimeter-scale obsidian pebbles, ca. 27 km due south of the Tsaghkunyats mountain range, and I used pXRF to confirm that these pebbles were Tsaghkunyats obsidian. Such tiny pebbles in secondary deposits have few implications for knapped lithic artifacts; however, it may explain how Tsaghkunyats obsidian fragments occasionally were incorporated into pottery as temper at a nearby Late Neolithic settlement (Palumbi et al., 2014).

3.2. Azerbaijan

Only one obsidian source occurs in the mountainous Nagorno-Karabakh region, which is disputed territory. Specifically, according to internationally recognized borders, the volcano falls just inside area of Azerbaijan; however, this territory is instead recognized by Armenia as the Republic of Artsakh. As with other obsidian sources that lie near contested national borders, this source has not been particularly well sampled or described in the literature due to its location and international politics.

3.2.1. Kelbadjar / Kechal Dağ

This obsidian source is known as Kelbadjar (sometimes transliterated as Kel'badjar, Kel'bedzhar, Kelbadzhar, etc.), Kechal Dağ (alternatively Kechaldağ, Kecheldağ, Kechel Dağ, etc.), and Merkasar (e.g., Keller et al., 1996; Blackman et al., 1998; Karapetian et al., 2001; Badalyan

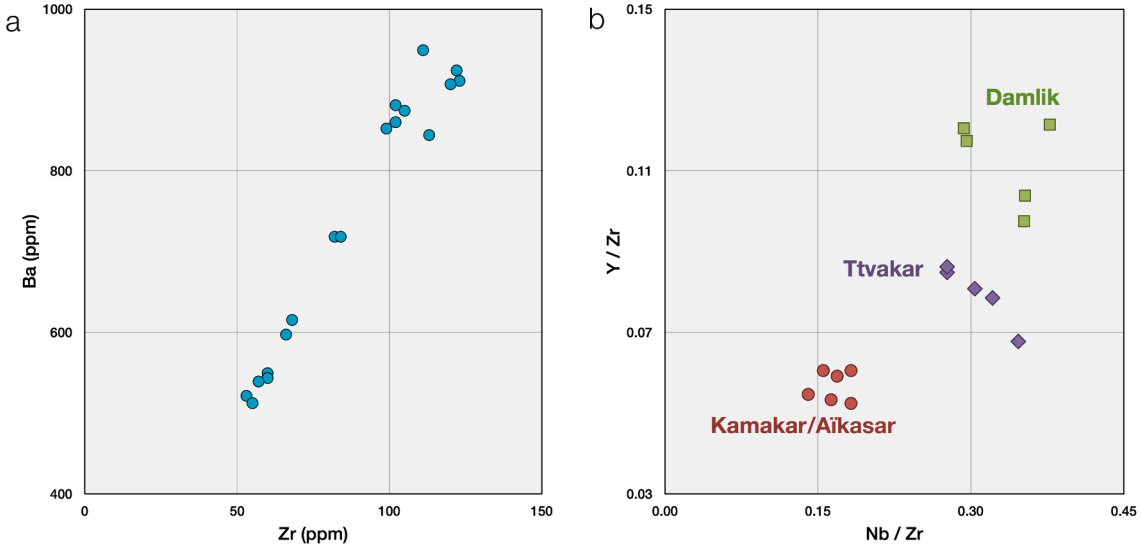

Fig. 13. Digitized scatterplots (using WebPlotDigitizer v 4.6) of LA-ICP-MS data for Tsaghkunyats obsidian from Chataigner and Gratuze (2014). (a) Chataigner and Gratuze (2014: 33) state "Tsaghkunyats obsidian forms two well-identified compositional groups" in their Ba vs. Zr plot, reproduced here. (b) Their Nb/Zr vs. Y/Zr plot, reproduced here, exhibits three distinct compositional groups, each of which corresponds to a known Tsaghkunyats obsidian source: Kamakar (which those authors combine with the Aïkasar deposit as their "Tsaghkunyats 2" subgroup), Ttvakar, and Damlik. Accordingly, their measurements support the same three obsidian sources that have identified by other researchers.

et al., 2004; Orange et al., 2021; Fataliyev et al., 2022). The first two terms are widely used in the recent obsidian literature (e.g., Orange et al., 2021; Fataliyev et al., 2022), so I simply use both names here. The obsidian outcrops (ca. 39.92° N, 45.87° E) lie at high elevations (ca. 3000–3200 m asl), which, in turn, leads to deep snow cover for more than half of the year (Badalyan et al., 2004). K–Ar dating at the volcano yielded an age of ca. 0.7 Ma (Keller et al., 1996). The obsidian occurs in association with extensive perlite and pumice deposits (Marakushev and Mamedov, 1993; Fataliyev et al., 2022), much like the Gutansar and Arteni sources.

Table S24 reports a single composition for this obsidian source, but it should be acknowledged that Blackman et al. (1998) claimed the existence of three source compositions, which they had termed Kecheldağ (n = 3 obsidian specimens), Kelbadzhar 1 (n = 4), and Kelbadzhar 2 (n = 1). They concluded, however, the Kecheldağ and Kelbadzhar 1 source are actually one and the same, and the compositional similarity of their one "Kelbadzhar 2" specimen to the nearby Khorapor obsidian source should not be ignored as mere chance (Blackman et al. 1998: Fig. 5). Instead, it likely was a misidentified specimen of Khorapor obsidian. Consequently, I, like my colleagues in this field (e.g., Orange et al., 2021; Fataliyev et al., 2022), propose that there is only a single Kelbadjar / Kechal Dağ obsidian source.

3.3. Georgia

Obsidian can only be collected from one lava dome in Georgia, located in the Djavakheti highlands, just 35 km from the northern border of Armenia. It should be noted, though, that other dark, aphanitic, likely volcanic toolstone materials occur among lithic artifacts excavated in Georgia (personal observations of the archaeological collections of the Georgian National Museum in Tbilisi).

3.3.1. Chikiani 1, 2, and 3

The Chikiani ("the glass that glistens" in Georgian) lava dome (41.48° N, 43.86° E; ca. 2200–2400 m asl) lies on the northeastern shore of Paravani Lake, and this source location is also known as Paravani (or Paravani Lake, Paravan, Paravana, Taparavani, etc.) and Kojun Dağ. Flows of high-quality obsidian (i.e., largely homogeneous and inclusion-free) occur across this low lava dome, which rises only 300 m above its surroundings, and quarries have been documented across the dome (Biagi and Gratuze, 2016; Biagi et al., 2017). Secondary alluvial deposits of obsidian clasts and pebbles have been reported along the course of the Khrami (Chrami) River to the east (Badalyan et al., 2004); however, large obsidian blocks are easily accessed at the dome and would have been reliable resources for those in search of excellent toolstone. Fission-track dating of Chikiani obsidian yielded ages between ca. 2.2 and 2.6 Ma (Komarov et al., 1972; Chataigner et al., 2003), whereas K–Ar dating yielded slightly older dates of ca. 2.4–2.8 Ma (Karapetian et al., 2001; Lebedev et al., 2008; Le Bourdonnec et al., 2012; Nomade et al., 2016). These date ranges do not necessarily mean that there was an extended, 400-ka period of rhyolitic volcanism, although this is a possibility to consider. Instead, these ranges might simply reflect reasonable uncertainties in these date determinations, especially in light of subsequent heating events (i.e., later eruptions) that, in theory, may have reset radiometric clocks and led to younger ages (Lebedev et al., 2008). There is chemical evidence of multiple obsidian-producing eruptions, but it is unclear how long this process took.

Some of the earlier studies (e.g., Blackman et al., 1998; Chataigner and Gratuze, 2014) reported a homogenous chemical composition among their tested Chikiani obsidian specimens. Keller et al. (1996), though, realized that a series of four obsidian specimens from Chikiani exhibited a linear, compositional trend reflective of magma at different stages of its chemical evolution. That is, obsidian erupted multiple times, between which the magma underground continued to change in composition, and the outcome is obsidian with a series of distinct trace-element compositions but that still constitutes a rather coherent geochemical group (Keller et al., 1996). Biagi and Gratuze (2016) later confirmed the presence of three trace-element compositions of Chikiani obsidian, which they numbered 1 through 3. Their precise spatial distributions across the landscape remain somewhat unclear, as most of the locations sampled by Biagi and Gratuze (2016) were colluvial deposits around the base of the lava dome. Biagi and Gratuze (2016) suggest that Chikiani 3 obsidian erupted first, meaning that the flow would be largely covered, and that Chikiani 1 obsidian, which occurs across the surface of the lava dome, erupted last.

Table S25, S26, and S27 summarize the compositional data for Chikiani 1, 2, and 3, respectively. Such a three-fold distinction is consistent with the most recent research from my colleagues in this field (e.g., Orange et al., 2021). It is worth noting that Biagi and Gratuze (2016) initially reported Chikiani 1a and 1b; however, only a short time later, they considered Chikiani 1b to instead be a part of Chikiani 2 (Biagi et al., 2017). Consequently, this distinction is not made here. In addition, Biagi and Gratuze (2016) make a distinction between Chikiani 3a and 3b. While such a subtle chemical difference might be possible for geological specimens with fresh, flat, and clean surfaces, making such a distinction non-destructively among artifacts is likely impractical. Hence, Chikiani 3a and 3b are combined here.

3.4. Russia

Most of the obsidian sources in Russia occur on the volcanic Kamchatka Peninsula of Siberia (e.g., Grebennikov and Kuzmin, 2017), but a single source also lies on the Russian side of the Greater Caucasus range in Kabardino-Balkaria, making it the only known source in the North Caucasus.

3.4.1. Baksan / Zayukovo

This obsidian source tends to be called Baksan (or alternatively Baksan River or Baksan Valley) by Western authors (e.g., Keller et al., 1996; Blackman et al., 1998; Le Bourdonnec et al., 2012) and Zayukovo by Russian authors (e.g., Doronicheva and Shackley, 2014; Shackley et al., 2018; Doronicheva et al., 2019), so Orange et al. (2021) has recommended the use of both terms together. Obsidian clasts are found in secondary alluvial, colluvial, and pyroclastic deposits along the Baksan River within the valley of the same name. For example, specimens analyzed by Shackley et al. (2018) were collected from slope deposits of undifferentiated Quaternary sediments. Although centered around the village of Zayukovo (43.6° N, 43.3° E), these clasts have been reported in relict river terraces and beds as much as 10 km away (Shackley et al., 2018). Most of the obsidian clasts are $\leq$ 10 cm in diameter and rarely are larger (Shackley et al., 2018). The river itself originates on the steep slopes of Mount Elbrus, a stratovolcano that is the highest peak of the North Caucasus (5640 m asl), but it might not be the geological source of the obsidian. The primary source remains unclear; however, it has been proposed that the eruptive center lies more than 40 km upstream from Zayukovo near the village of Tyrnyauz (43.4° N, 42.9° E) based on volcanism of similar age within the immediate vicinity (Le Bourdonnec et al., 2012; Shackley et al., 2018). Specifically, fission-track dating of the obsidian yielded an age of 2.2 ± 0.2 Ma (Komarov et al., 1972), while nearby granite massifs have similar ages (e.g., 2.1–2.5 Ma in Hess et al., 1993; 2.0 ± 0.2 Ma in Borsuk, 1979). Table S28 shows, in agreement with colleagues in this field (Le Bourdonnec et al., 2012; Shackley et al., 2018), that, despite a variable appearance, there is a single composition of Baksan / Zayukovo obsidian.

3.5. Turkey

As previously noted, the area that is now eastern Turkey constitutes the geographic focus of this section. This region is often called Eastern Anatolia in the obsidian literature, following the terminology first laid out by Renfrew et al. (1969). The obsidian-producing volcanoes in

central Turkey are, in contrast, known as the Central Anatolian or Cappadocian obsidian sources, and they lie within an area termed the Central Anatolian Volcanic Province. Poidevin (1998) covered these sources in greater detail, and these sources, especially those of the Göllü Dağ complex, have been well described elsewhere in the literature (e.g., Hancock and Carter, 2010; Poupeau et al., 2010; Binder et al., 2011). This section also ignores the few small, old (20–25 Ma), and only locally exploited sources in western Turkey.

3.5.1. Bingöl a (Solhan)

Bingöl A is one of only two peralkaline obsidian sources in Southwest Asia and, accordingly, was included within the "Group 4c" obsidian of Renfrew et al. (1966). Alkaline obsidian is more common, and in comparison, peralkaline obsidian has lower Al contents as well as higher concentrations of Fe and alkali elements such as Na and K. Trace-element trends also differ between the two geochemical varieties. Ba and Sr are higher in alkaline obsidian, while peralkaline obsidian has higher Nb and Zr contents. This is a result of different minerals that form in the magma. In alkaline obsidian, the formation of zircon ($ZrSiO_4$) and other minerals in the magma leads to low Zr concentrations left behind in the glass, whereas these minerals do not form in peralkaline magmas, leading to higher Zr levels within the resulting obsidian. In contrast, Ba and Sr can be high in alkaline obsidian, but feldspars that form in peralkaline magmas readily accept Ba and Sr into their crystal structure and, in turn, reduce their levels in the resulting obsidian. The different trace-element trends for peralkaline obsidian not only obfuscated that there is more than one source in Southwest Asia but also complicated efforts to differentiate them.

Cauvin (1991) coined the term Bingöl A to describe the peralkaline obsidian found near the city of Bingöl and belonging to the Solhan formation (Yilmaz et al., 1987). This obsidian is associated with two principal exposures that are known in the literature as Orta Düz (ca. 38.92° N, 40.91° E, 1300 m asl) and Çavuşlar (ca. 38.93° N, 40.75° E, ca. 1400 m asl). The Orta Düz deposit is an obsidian layer, about 1 m thick, that is exposed in a road cut along the main route between the cities of Bingöl and Muş. The layer, which appears to be a primary deposit (and is the reason why this source is sometimes known instead as Solhan), sits atop volcanic tuff, and it is capped by a subsequent basalt flow, which is why the location of the Bingöl A primary deposit remained uncertain for so long. Çavuşlar, in contrast, is a secondary deposit of rounded, even spherical, obsidian clasts (ca. 10–25 cm in diameter) due to reworking by water and/or mud, and these clasts occur in various accumulations in the area around the town of Çavuşlar, typically where hill slopes have concentrated them together. Bingöl A obsidian has been fission-track dated to ca. 4.6–5.1 Ma (Bigazzi et al., 1998; Bellot-Gurlet et al., 1999) and K-Ar dated to ca. 4.2–4.6 Ma (Chataigner et al., 1998). Table S29 summarizes the available elemental data for Bingöl A obsidian.

3.5.2. Bingöl B (Alatepe)

Cauvin (1991) also coined the term Bingöl B in order to describe the alkaline obsidian that occurs near the city of Bingöl. It was known as "Group 1g" in the work of Renfrew et al. (1966) when its source locale was unknown, but its deposits were discovered by surveys that archaeologist Marie-Claire Cauvin organized during the 1980s. The Alatepe exposure (ca. 39.15° N, 40.77° E, 1700 m asl) has been described as a small obsidian flow, and it appears to be a primary source of Bingöl B obsidian. There are two known secondary deposits of obsidian clasts that have been reworked by streams and/or mudflows: one near the village of Çatak, where rounded clasts as large as 30 cm across occur in association with fluvial sediments, and another deposit near the village of Arçük. Bingöl B obsidian has been fission-track dated to ca. 4.3–6.0 Ma (Bigazzi et al., 1998) and K-Ar dated to ca. 4.4–4.7 Ma (Chataigner et al., 1998). Table S30 summarizes elemental data for Bingöl B obsidian from the 1980s onward.

3.5.3. Erzincan 1 and 2

Two lava domes, about 10 km apart, east of the town of Erzincan produced obsidian with similar elemental compositions: Erzincan 1 obsidian from a lava dome called Agili Tepe (Table S31) and Erzincan 2 obsidian from a dome called Değirimen Tepe (Table S32). Volcanism within the Erzincan basin appears to be directly related to the North Anatolian and Northeast Anatolian crustal faults at this location, and other domes nearby erupted dacite and rhyodacite lavas. Agili Tepe lies near the village of Karakaya (also called Keleriç; ca. 39.68° N, 39.75° E, 1400 m asl), and Değirimen Tepe is near the village of Çadırtepe (or Kertah; ca. 39.71° N, 39.66° E, 1200 m asl). Ar-Ar dating of obsidian and dacite implies an age between ca. 0.4 ± 0.2 and 0.5 ± 0.2 Ma (Poidevin, 1998), but additional dating is still needed.

3.5.4. Erzurum: Tambura, South Erzurum, and West Erzurum 1 and 2

The Erzurum Province contains, by my count, four distinct obsidian compositions, the deposits of which were first documented by Pasquarè (1971). Erzurum–Tambura (Table S33) obsidian derives from the pyroclastic deposits of a particular cinder cone within the Kilbe Tepe volcanic system, near the village of Güzelyurt (previously called Tambura; ca. 39.8° N, 41.0° E, 1900 m asl). Bigazzi et al. (1998) determined a fission-track age of ca. 6.9 ± 0.3 Ma for these pyroclastics, but the uncertainties involving this date are unclear. Furthermore, based on their own visit, Kobayashi and Sagona (2008) thought that this material was too granular and low-quality to have been useful for tool-making during the past, and Chataigner et al. (2014) remark that they were unable to locate obsidian during their survey.

South Erzurum obsidian (Table S34) apparently derives from Kuşakli Dağ volcano to the west of the town of Başköy (ca. 39.717° N, 41.136° E, 2300 m asl). Pasquarè (1971: 905) describes this source as exhibiting a sequence of "vitreous laminated tufts, among which, however, some layer[s] up to 15–20 cm thick are made up entirely of pure obsidian." Opaque, black obsidian outcrops at multiple places across the volcano (Chataigner et al., 2014). So far, a total of only four geological specimens of South Erzurum obsidian have been analyzed using LA-ICP-MS in Orléans (Chataigner et al., 2014) and using pXRF in the archaeological labs of the University of California-Los Angeles (Olshansky, 2018), and a matching artifact from İvikler Tepsei was also measured using NAA in Australia (Brennan, 2000).

West Erzurum 1 obsidian (Table S35) derives from Güney Dağ volcano (ca. 39.9° N, 41.1° E, 1900–2000 m asl) immediately to the west of the villages of Sögütlü and Ömertepe. Angular blocks of obsidian are scattered across the surface but not in situ. Instead, the blocks seem to have somewhat moved from their initial emplacement contexts due to an explosive eruption (consistent with a circular depression), a pyroclastic flow (consistent with the associated pumiceous/perlitic deposits), and/or freeze–thaw cycles (Poidevin, 1998). Domes of dacitic lava also dot the volcano's surface. One Ar-Ar date yielded an age of 8.4 Ma, consistent with Miocene-aged obsidian in this province (Poidevin, 1998).

West Erzurum 2 obsidian (Table S36) has a less clear volcanic origin, but its specimens appear to have been collected near West Erzurum 1 specimens. A distinct possibility is that secondary deposits of water-rounded obsidian clasts along Adaçay River near Ömertepe village were presumed to derive from Güney Dağ volcano but instead originate farther upstream, such as the Palandöken Dağları volcanic ridge (Brennan, 2000). Other secondary deposits have also been noted farther downstream, such as one near the village of Aziziye (previously known as Ilıca) (Poidevin, 1998). Clearly, the Erzurum Province is one of the regions that requires more work to better circumscribe its obsidian sources.

3.5.5. Group 3d

The term "Group 3d" comes from Renfrew et al. (1966), who identified artifacts with notably high Rb concentrations (450–500 ppm vs. less than 300 ppm for other sources) but did not find a matching

geological source. Today the source remains unknown – no one knows precisely where past peoples collected this obsidian. For decades, only a handful of Group 3d obsidian artifacts had been identified. These sites had other artifacts principally from obsidian sources in the vicinity of Lake Van (e.g., Bingöl A and B, Nemrut Dağ, Meydan Dağ), providing a few clues about its location. For decades, however, this source remained something of a boogeyman. Campbell and Healey (2016) revolutionized our understanding of this source when, using pXRF, they identified 278 Group 3d artifacts (31.5% of the tested assemblage) from the site of Kenan Tepe (37.831° N, 40.813° E, 550 m asl), which lies on the Tigris River in the Diyarbakır Province of southeastern Turkey. Other obsidian artifacts at Kenan Tepe (e.g., 122 from Bingöl A, 122 from Bingöl B, and 339 from Nemrut Dağ, but many fewer from other sources) implies a source located somewhere between those three sources and the site. Furthermore, Campbell et al. (2020) summarize the available information about Group 3d obsidian, and interested readers are encouraged to consult that publication and its references. Table S37 lists the elemental data for Group 3d obsidian.

3.5.6. *İkizdere*

İkizdere obsidian derives from a large source (6-km long, ca. 40.8° N, 40.7° E, 1800–2800 m asl), known as Haros Dağ, near the towns of İkizdere, Rize, and Büyük Yayla (Yeğingil et al., 2002). There are several named obsidian exposures, including Büyüksulata and Kücüksulata (western exposures), Büyük Yayla (central), and Tekem Tepe and Kara Tepe (eastern); however, the various exposures exhibit a very consistent chemical composition (Yeğingil et al., 2002), as summarized in Table S38. Yeğingil et al. (2002) propose that the obsidian had an atypical emplacement mechanism, arguing that it filled faults initiated by a regional Pliocene neotectonic fracture system. This process, however, led to obsidian with vesicles (bubbles), millimeter-scale inclusions of biotite and feldspar, and partially devitrified glass, which limited its utility for lithic production in the past. Nishiaki et al. (2019) refer to a "Group 1" (n = 2) and "Group 2" (n = 5) of İkizdere obsidian, but this distinction is based, in large part, on differences between the Ti (843 ± 48 and 1009 ± 33 ppm, respectively) and Fe (6334 ± 206 and 7474 ± 260 ppm) contents. As discussed in Section 2, variations in the abundance of magnetite ($Fe^{2+}Fe^{3+}_2O_4$), titanomagnetite ($Fe^{2+}(Fe^{3+},Ti)_2O_4$), or ilmenite ($FeTiO_3$) can lead to spurious groups in otherwise homogeneous obsidian. İkizdere obsidian has been fission-track dated to ca. 1.7–1.9 Ma and K-Ar dated to ca. 2.10 ± 0.03 Ma (Yeğingil et al., 2002). It should be mentioned that, in their unpublished study of İkizdere obsidian, Weiss et al. (2002) reported a distinct composition for three obsidian specimens collected from Sehitlik peak, southeast of the İkizdere exposures. Importantly, two subsequent studies, also unpublished and lesser known, suggested that the specimens were not actually obsidian but instead tektites, which are natural glasses formed from molten ejecta during meteorite impacts (Kloess et al., 2003; Ende et al., 2007).

3.5.7. *Kars: Akbaba Dağ, Arpaçay 1 and 2, and Digor 1 and 2*

The Kars Province of northeast Turkey includes a series of Plio-Pleistocene tuffs, ignimbrites, and pyroclastic deposits that contain obsidian, which have also been transported by alluvial mechanisms in the region. Consequently, secondary deposits of water-transported obsidian clasts also occur across this province, and this, in turn, has led to different nomenclatures used by various researchers. Here I follow the terminology used by volcanologist Tuncay Ercan and colleagues with Turkey's Directorate of Mineral Research and Exploration and later employed by Keller et al. (1996). I do, though, report equivalences to later authors' nomenclature (e.g., Chataigner et al., 2014) whenever possible.

About 15 km south of the town of Kars, Kars–Akbaba Dağ (ca. 40.497° N, 43.021° E, 2000 m asl) obsidian was sampled in 1991 by Ercan and colleagues. No dates are available for this source, but those for other Kars obsidian sources (below) suggest that their emplacement occurred during a volcanic phase between ca. 2 and 4 Ma. Elemental scatterplots in Keller et al. (1996) include NAA measurements of this obsidian by Pernicka and Keller; however, these data were not otherwise published. My analyses of this particular obsidian source (Table S39) appear to be the only published values.

Kars–Arpaçay 1 (Table S40) and Kars–Arpaçay 2 (Table S41) obsidian were sampled by Ercan and colleagues to the northwest and southwest, respectively, of the village of Büyük Aküzüm (ca. 40.65° N, 43.66° E, 1500 m asl). This village lies near the confluence of the Kars and Aparçay (or Akhurian) Rivers, and the specimens were collected from secondary alluvial deposits. Specimens of Kars–Arpaçay obsidian (unknown if they were Kars–Arpaçay 1 and/or 2) have been fission-track dated to ca. 3.5 ± 0.2 and 3.7 ± 0.2 Ma (Bigazzi et al., 1998). Kars–Arpaçay 1 is equivalent to both the "Akhurian" and "Sarıkamış North" sources of Chataigner and Gratuze (2014). It should be pointed out that Chataigner and Gratuze (2014) also subdivide their specimens into Akhurian 1 (n = 2) and Akhurian 2 (n = 12) based on a relatively minor difference in Ba content (95 ± 14 vs. 29 ± 5 ppm, respectively). I do not, however, make such a distinction here. Clearly the volcanic origin of Kars–Arpaçay 1 obsidian lies upstream, but exactly where remains a matter of debate (Poidevin, 1998: 133; Chataigner and Gratuze, 2014: 34–35).

In contrast to Kars–Arpaçay 1 obsidian, Kars–Arpaçay 2 obsidian has no equivalent in Chataigner and Gratuze (2014). Like Kars–Akbaba Dağ, elemental scatterplots shown in Keller et al. (1996) include NAA measurements from Pernicka and Keller of both Kars–Arpaçay 1 and 2 obsidian (which they instead call Kars–Arpaçay A and B); however, these data were not otherwise published. Therefore, also like Kars–Akbaba Dağ, my analyses (Table S41) appear to be the only published values.

Kars–Digor 1 (Table S42) and Kars–Digor 2 (Table S43) are equivalent to the Yağlica Summit (ca. 40.24° N, 43.33° E, 2100 m asl) and Yağlica South (ca. 40.21° N, 43.31° E, 1800 m asl) obsidian sources, respectively, of Chataigner et al. (2014). Specimens of Kars–Digor obsidian (unknown if they were Kars–Digor 1 and/or 2) were fission-track dated to 2.4 ± 0.2 Ma (Bigazzi et al., 1998) and Ar-Ar dated to 2.7 ± 0.3 Ma (Innocenti et al., 1982), reflecting the expected Plio-Pleistocene age.

3.5.8. *Meydan Dağ*

On the eastern slopes of Meydan Dağ volcano, obsidian outcrops are visible on a hillside known locally as Gügürbaba Tepe (39.204° N, 43.269° E, 2000 m asl). Older terms found in the literature for this source include Ziyaret (e.g., Fornaseri et al., 1975) and Zarnaki (or Zernaki) Tepe (e.g., Yellin and Perlman, 1981), the latter of which is the name of a nearby archaeological site from which obsidian artifacts were collected for chemical analysis. Gügürbaba Tepe appears to be a typical rhyolitic lava dome, in which the obsidian is capped by a perlitic/pumiceous layer, on the lower flanks of a Plio-Pleistocene stratovolcano. It does not seem that obsidian is directly associated with the volcanic caldera atop Meydan Dağ. Based on K-Ar dating of other lavas, the main volcano-building phase occurred between 6.2 and 4.6 Ma (Innocent et al., 1976). The obsidian, in contrast, is fission-track dated to ca. 0.75–0.60 Ma (Bigazzi et al., 1998) and K-Ar dated to ca. 1.0–0.9 Ma (Innocenti et al., 1980; Matsuda, 1988). Therefore, obsidian emplacement occurred millions of years later than the majority of the volcano. Table S44 summarizes the available data for Meydan Dağ obsidian, which, as an obsidian standard used for pXRF calibration (see Frahm, 2019 and references within), has been well characterized in a variety of laboratories.

3.5.9. *Muş*

The Muş (or Mush) Depression contains a sequence of sediments and volcanics, including a lava dome (38.893° N, 41.404° E, 1300 m asl) in the Zirnak Formation about 9 km southwest of the village of Mercimekkale (Yilmaz et al., 1987; Pearce et al., 1990; Ercan et al., 1995). A

mistake (i.e., field notes that stated "20 km *NW* of Mush town" instead of the correct *NE*) led some authors (e.g., Bigazzi et al., 1998; Poidevin, 1998), including myself (Frahm, 2010), to erroneously state that there are two sources of Muş obsidian. There is, though, only the one dome and its outcrops. Muş obsidian has been fission-track dated to ca. 2.0–2.7 Ma (Bigazzi et al., 1998), and Table S45 gives its composition.

3.5.10. *Nemrut Dağ 1 through 6*

Nemrut Dağ volcano (38.622° N, 42.243° E, ca. 2000–2400 m asl) is the other volcanic source of peralkaline obsidian in Southwest Asia, and its obsidian was also part of the "Group 4c" of Renfrew et al. (1966). Entire papers have been written about the geology (e.g., Aydar et al., 2003; Karaoğlu et al., 2005:; Özdemir et al., 2006; Çubukçu et al., 2012; Ulusoy et al., 2019) and obsidian (e.g., Frahm, 2012; Robin et al., 2015, 2016) of Nemrut Dağ since Poidevin (1998), and interested readers are especially encouraged to consult Frahm (2020) and the references therein for the most up-to-date information. Nemrut Dağ is an active stratovolcano, and it experienced a caldera collapse ca. 270 ka, creating a roughly circular, 7 × 8 km crater with a lake in its western half and subsequent lava flows and domes in its eastern half. There was obsidian produced both before and after the caldera collapse event. The oldest obsidian, exposed in the caldera wall, has been K-Ar dated to ca. 310 ka (Özdemir et al., 2006), whereas the youngest obsidian on the caldera floor has been fission-track dated to ca. 24 ± 14 ka (Bigazzi et al., 1998) and K-Ar dated to ca. 20–25 ka (Matsuda, 1988; Notsu et al., 1995). To be brief here, early analyses of Nemrut Dağ obsidian involved too few specimens and little or no location information for them, and it was unclear how many distinct obsidian compositions occurred at the volcano. The issue was complicated by real compositional variability attributed to analytical uncertainties and inter-laboratory offsets. In general, it was held that there were two or perhaps three obsidian compositions at Nemrut Dağ when I first identified six distinct compositions (Frahm, 2010, 2012). Others have since been able to replicate my results (e.g., Robin et al., 2016). Table S46 to S51 summarize all of the available data. Following Robin et al. (2016), who showed that most (but not all) Nemrut Dağ obsidian artifacts match the Nemrut Dağ 2 source, called Cluster 2 in Frahm (2020) and Cluster 2 / Outcrop 5 / Sıcaksu in Robin et al. (2016), I chose to include all artifact data in the Nemrut Dağ 2 table here because even a few artifacts from other Nemrut Dağ sources (see Frahm, 2020) would only have a minor influence on the resulting mean values.

3.5.11. *Pasinler 1 and 2*

The name "Pasinler" derives from the initial identification of obsidian clasts in river gravels near the town of Pasinler, followed by geochemically matching obsidian artifacts from the archaeological site of Sos Hüyük ca. 13 km west of Pasinler (Brennan, 2000). The volcanic origin of the clasts, however, was unknown as of Poidevin's (1998) chapter. Later obsidian outcrops were found, ca. 14 km to the north, on the east bank of the Malikom River (or Büyükdere) Gorge (Fig. 14; 40.067° N, 41.617° E, ca. 1800–2000 m asl). It was this river that transported the obsidian clasts south to Pasinler. Brennan (2000: 132) describes the Malikom Gorge exposure as "at least five discrete flows of obsidian, each up to several meters thick" that are "inter-bedded with obsidian-rich tuffs." His description does not necessarily mean that there are five or more different compositions of obsidian present there; however, it seems likely that both Pasinler 1 and 2 obsidian originate from these outcrops. Pasinler obsidian has been fission-track dated to ca. 5.5–6.2 Ma (Bigazzi et al., 1998) and Ar-Ar dated to ca. 5.5 ± 0.1 Ma (Chataigner et al., 1998). Table S52 and S53 summarize the available data for Pasinler 1 and 2 obsidian, respectively.

3.5.12. *Sarıkamış 1, 1a, and 2*

The Sarıkamış district of northeastern Turkey includes several obsidian deposits, and it has been debated precisely how many chemically different sources are among them. On the low end of the source number, some authors propose that there are two sources (e.g., Sarıkamış 1 and 2 in Keller and Seifried, 1990; Sarıkamış South 1 and 2 in Chataigner and Gratuze, 2014). On the high end, Gratuze et al. (2022) hold that there are as many as five chemically distinct obsidian sources (i.e., Sarıkamış South 1A, 1B, 1C, 2A, and 2B). I, however, concur with my colleagues with the GéObs Project and the Manchester Obsidian Lab that Sarıkamış obsidian is best sorted into three sources (e.g., Nishiaki et al., 2019). My sources also correlate with those of Gratuze et al. (2022): my Sarıkamış 1 obsidian (Table S54) is their Sarıkamış South 1C obsidian, my Sarıkamış 1a (Table S55) is their Sarıkamış South 1A, and my Sarıkamış 2 (Table S56) is their Sarıkamış South 2A and 2B, whereas their Sarıkamış South 1B reflects outliers. Sarıkamış 1 obsidian originates from the slopes of Ala Dağ (40.270° N, 42.721°, ca. 2200–2700 m asl), right between Hamamlı village to the north and Şehitemin village to the south. It may be that Sarıkamış 1a obsidian also derives from this area, but precisely circumscribing it on the landscape remains challenging. Sarıkamış 2 obsidian originates from Çiplak Dağ, and it is exposed in various cuts (e.g., 40.214° N, 42.651° E, 1800 m asl) along the Erzurum–Kars road near the village of Mescitli. Six Sarıkamış obsidian specimens have been fission-track dated between ca. 3.6 ± 0.2 and 4.8 ± 0.3 Ma (Bigazzi et al., 1998), and this spread of approximately a million years may reflect the ages of these different sources (Poidevin, 1998).

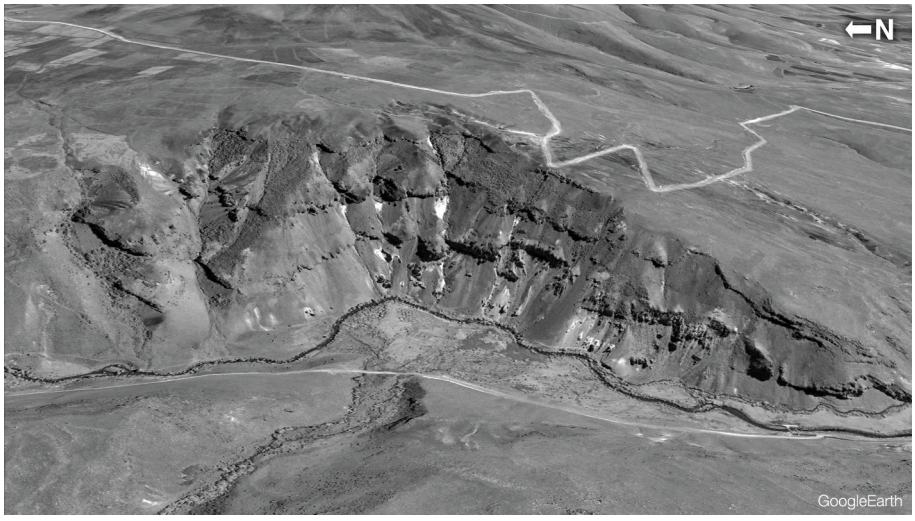

Fig. 14. Obsidian outcrops, ca. 14 km north of Pasinler village, on the eastern bank of the Malikom River Gorge. Brennan (2000: 132) describes this exposure as "at least five discrete flows of obsidian, each up to several meters thick" that are "inter-bedded with obsidian-rich tuffs." Pasinler 1 and 2 obsidian may both originate from these outcrops. The Google Earth image is reproduced here in accordance with Google's Terms of Service and General Guidelines regarding fair use in publications (©2023, Maxar Technologies, imagery collected on 27 June 2011).

3.5.13. Süphan Dağ 1 and 2

Süphan Dağ (38.93° N, 42.81° E, summit at ca. 4000 m asl) is a polygenetic stratovolcano, located where two major fault lines intersect and with a complicated eruptive history. In brief, various dates on lavas and obsidian suggest that the major volcano-building phase occurred between ca. 0.7 and 0.1 Ma, whereas obsidian formed at or near the end of this process ca. 680 ± 12 ka (Innocenti et al., 1976; Pearce et al., 1990; Notsu et al., 1995; Bigazzi et al., 1998). Its obsidian has very rarely, if ever, been identified at archaeological sites, mostly likely due to its frequent porphyritic texture (i.e., silicate minerals, primarily plagioclase, visible to the unaided eye) and, in turn, lower knapping quality (Poidevin, 1998). Blackman (1984) identified two Süphan Dağ obsidian compositions, which he termed Süphan I and II, and Oddone et al. (1997) corroborated the two distinct compositions, although other authors did not. Indeed, others seem only to have analyzed Blackman's "Süphan II" obsidian, which occurs in a different location on the volcano. Süphan Dağ 1 obsidian (Table S57; Blackman's "Süphan I") apparently originates from a flow on the southwestern slope (38.92° N, 42.78° E, ca. 3100 m asl), while Süphan Dağ 2 (Table S58; Blackman's "Süphan II") occurs on the northern slope (38.96° N, 42.81° E, ca. 2700 m asl).

3.6. Volcanoes misidentified as obsidian sources

Elsewhere I have addressed erroneous obsidian sources reported in Armenia (i.e., the purported "Erevan" and "Sevan" sources in the 1990 s literature; Frahm et al., 2016: 546–547); however, there are also two volcanoes in far eastern Turkey – Mount Ararat and Tendürek Dağ – sometimes reported to be obsidian sources but without chemical data that support such an interpretation.

3.6.1. Mount Ararat

Mount Ararat (also Ağrı Dağ) is a compound, polygenic stratovolcano that covers ca. 1100 km^2 near the borders of Turkey, Armenia, Iran, and Nakhchivan. As detailed by Yilmaz et al. (1998), volcanism started with a period of Plinian (Vesuvius-like) fissure eruptions that deposited ca. 700 m of pyroclastics and basalt flows, followed by a cone-building phase of successive andesite, dacite, and basalt lavas and pyroclastic flows. The double peaks of Mount Ararat were formed during a period of abundant andesite and basalt lava flows. The final phase of volcanism involved eruptions from fissures and cracks along the flanks, creating parasitic domes and cones, at least one of which erupted extensive andesite and basalt lava flows that led to 'a'ā and pāhoehoe morphologies. Rhyolite lavas are rare, largely restricted to small lava domes and flows on the western flank due to this final volcanic phase. Yilmaz et al. (1998) mapped no obsidian at this volcano, only two small lava flows of aphanitic andesite.

It was common for 19th-century geologists and explorers, including Jean-Jacques de Morgan, to write about fields of obsidian at Mount Ararat, which almost certainly were the lithic scatters associated with open-air Palaeolithic sites. Such ideas have been written about ever since (e.g., "obsidian flows from the twin peaks of Mt. Ararat," Moorey, 1999: 66; "obsidian mining on the slopes of Mount Ararat," Ali, 2009: 22). About a third of the obsidian source specimens analyzed by Renfrew et al. (1966) came from the Natural History Museum in London (hereafter NHMUK), which was known as the British Museum of Natural History until the 1960s. Their Mineralogy and Planetary Sciences Division collection includes one specimen of banded obsidian reportedly from Mount Ararat: catalog numbers BM.1955,309 and NHMUK 268656. This number indicates that the specimen was accessioned by the museum in 1955, and the web catalog lists "G. Brown" as its donor. The NHMUK sent me a subsample of this "Mount Ararat" obsidian for nondestructive testing. Table S59 reveals that this specimen is actually Gutansar obsidian, indicating that an anthropogenic context, likely an archaeological site, was sampled.

3.6.2. Tendürek Dağ / Bayezid

Tendürek Dağ is a polygenetic shield volcano southwest of the town of Doğubeyazıt (previously known as Bayezid), and its eastern flows almost reach the border with Iran, which has long complicated field research there. The lavas of Tendürek Dağ are principally basalts and trachyandesites (Innocenti et al., 1976; Pearce et al., 1990), but this volcano has periodically been mentioned within the literature as a potential obsidian source. A geological map reproduced by Yilmaz et al. (1998: Fig. 4) likely dates to the 1980s, if not earlier, and it shows an obsidian flow immediately east of the village of Esnemez (39.46° N, 43.91° E, ca. 2000 m asl). There is clearly a lava flow adjacent to the village, but there are no indications of obsidian outcrops in either ground or satellite photography. Furthermore, three procurement visits by experienced researchers failed to locate any primary source deposits. Instead, in each case, an alluvial secondary deposit or archaeological lithic scatter were sampled instead.

Specimens of "Tendürek Dağ" obsidian were collected by Tuncay Ercan and/or colleagues in the Directorate of Mineral Research and Exploration. Their field notes are consistent with the location of the purported obsidian deposit (Yilmaz et al., 1998) and also state that obsidian was "rare" there. I analyzed these specimens using EMPA (Frahm, 2010), and it was only later that I understood those specimens fall in the normal variability of Meydan Dağ obsidian (Table S60). That is, this "rare" obsidian appears to have come from a lithic scatter atop the lava flow, and the artifacts instead derived from Meydan Dağ, one of the most widely and intensively exploited obsidian sources in the region.

USGS volcanologist Robert L. Smith, who helped to develop obsidian hydration dating during the 1950s and 1960s, assembled a large obsidian collection, which was either divided or shared between the NHMUK and the Smithsonian Institution's Lithological Reference Collection in Washington, D.C. Obsidian specimens in these museums' collections share British Museum (BM), NHMUK, and Smithsonian numbers as well as field sample numbers and International Generic Sample Numbers (IGSNs), as I have described previously (Frahm et al., 2016: 547). Tendürek Dağ is often proposed as the likely source for a "Bayezid" obsidian specimen analyzed by Renfrew et al. (1966), which is listed in the NHMUK catalog as "part of a water-worn stone" from "Bayezid." This specimen has the catalog numbers BM.93035, NHMUK 248789, and NMNH (Smithsonian) 117451–16 as well as the field number EA 3–5-2 and IGSN NHB007464. This is consistent with other specimens from Smith's obsidian collection. The Smithsonian loaned me either the same specimen analyzed by Renfrew et al. (1966) or a matched sample. Fig. 15 shows that it is a wedge-shaped flake from a water-rounded obsidian clast, as described. My new analyses, alongside those from Renfrew et al. (1966), reveal its affinity to Pasinler 2 obsidian (Table S60). Presumably this specimen was collected from a secondary deposit downstream from the Pasinler sources.

Using LA-ICP-MS in Orléans (France), Chataigner and Gratuze (2014: 41) analyzed "Tendürek Dağ" obsidian specimens, which were forwarded from M.D. Glascock at MURR and originate from a "flat area on the eastern flank" of the volcano, not the lava flow from the geological map reproduced by Yilmaz et al. (1998). That is, the specimens derived from a secondary deposit, not a primary outcrop. Glascock did not collect these specimens. Instead, they were sent to MURR by M. James Blackman of the Smithsonian Institution's Conservation Analytical Laboratory. Blackman (1984; Blackman et al., 1998; Blackman and Bishop, 2007) is, of course, known for characterizing Near Eastern obsidian sources using NAA. Blackman et al. (1998: 213) note that the specimens were "collected from [a] stream deposit near the near the city of Doğubayazıt," meaning that the "source samples" came from an alluvial context. Table S60 shows that (1), taking into account the considerable differences between the two analytical techniques, the obsidian compositions appear fairly consistent between the labs and (2) the "Tendürek Dağ" obsidian specimens exhibit a chemical affinity to Sarıkamış 1 and 1a obsidian. Therefore, it seems reasonable to conclude that Blackman and colleagues sampled an alluvial deposit of Sarıkamış

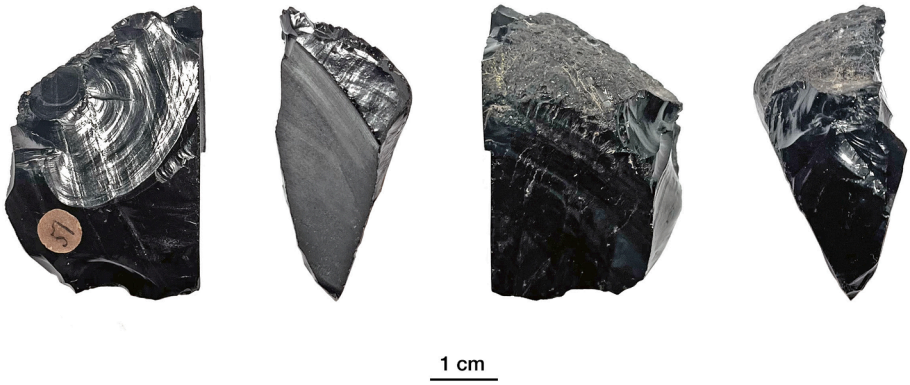

Fig. 15. The "Bayezid" obsidian specimen (NMNH 117451–16, IGSN NHB007464, field number EA 3–5-2) in the Lithological Reference Collection of the Smithsonian Institution (Washington, D.C.). This piece from a water-rounded obsidian clast either is the same specimen that was analyzed by Renfrew et al. (1966) or a matched sample. Note that a rock saw has previously been used at some point to remove material for analysis, potentially that of Renfrew et al. (1966). As discussed in Section 3.5.14, my pXRF analysis of this specimen establishes that it is chemically consistent with Pasinler 2 obsidian.

obsidian.

In short, Meydan Dağ, Pasinler, and Sarıkamış obsidian were collected from locales purported to be near an obsidian flow of Tendürek Dağ. That flow, however, is known only from a greater than 40-year-old map of the shield volcano, not an obsidian-focused source survey. Furthermore, those specimens from Smith and from Blackman came from explicitly secondary deposits, not outcrops. Therefore, I would argue that, if there is indeed autochthonous obsidian at Tendürek Dağ, it has not yet been chemically characterized and published, and until then, it should not be listed among known sources.

4. Concluding remarks

At the end of his chapter, Poidevin (1998: 152) remarked that his database was almost certainly incomplete, especially concerning small, inaccessible, or otherwise obscure obsidian sources that might have seen only local utilization. He emphasized the importance of systematic regional surveys and cited northeastern Turkey as an area that was particularly lacking ("In northeastern Turkey, almost everything remains to be done," translated from French). Progress has been made in this regard (e.g., Brennan, 2000; Chataigner et al., 2014), but this region remains one with a high potential for unknown obsidian sources, which might correspond to occasional unidentified artifacts in the literature. Geology, he observed, does not follow national borders, so researchers would ideally follow geological realities more than arbitrary political boundaries. After compiling all of the available data, Poidevin (1998: 152) commented that, at that time, obsidian source characterization reflected "multiple approaches" and, hence, was "extremely messy" [translated from French]. In particular, he stated that, with such limited data, he had to list "the very good alongside the more mediocre, if not useless" [translated from French]. Ultimately his chapter ends with Poidevin's (1998: 153) call for "the acquisition of new data [regarding] the characterization of obsidian" [translated from French] to further enhance artifact sourcing.

Here I have endeavored to bring order to the "mess" and remove inaccurate measurements, for whatever reason, in order to derive useful consensus values – or, more correctly, consensus ranges – for the elemental data. The geographic range of this database reflects a specific geological context, namely the Caucasian segment of the Alpine-Himalayan belt. Assembling these data from multiple independent analytical techniques and facilities has allowed for better recognition of outliers and greater confidence in accuracy of the averaged values. As discussed in the Introduction, my aim is to be comprehensive, not authoritative, and it might not be that other experts agree with all of the choices that I made during the process of assembling this database. For this reason, I provide the lab-by-lab breakdown of the analytical data used to determine the consensus values for each obsidian source, and the full references enable a reader to find details, including calibration protocols and accuracy evaluations, regarding each analytical technique and laboratory. It is my sincere hope that this database will be as useful to current and future archaeologists as Poidevin's (1998) chapter was to me and other researchers in this field for the last two decades. Additionally, I hope that this article serves as a model for obsidian specialists in other regions to assemble, summarize, and share the datasets for their parts of the world.

Declaration of Competing Interest

The author is an editor-in-chief for the journal. He was not, though, involved in decisions regarding its publication, and he was blinded to the review process since the manuscript was handed by a different editor. There are no other known competing interests or relationships that could have appeared to influence the work reported in this paper.

Data availability

The data are included in the supplementary tables

Acknowledgements

An endeavor such as this one does not occur in a vacuum, and I began this research literally 20 years ago during my first year as a doctoral student at the University of Minnesota-Twin Cities. Consequently, I am indebted to many friends and colleagues who, in a multitude of ways, made this work possible. Allow me to apologize in advance if I have overlooked anyone here. Although I collected many of the geological obsidian specimens myself, additional specimens were provided by (in alphabetical order): Ruben Badalyan (Institute of Archaeology and Ethnography, National Academy of Sciences, Armenia), Giulio Bigazzi (Institute of Geochronology and Isotope Geochemistry, Italy), M. James Blackman (Smithsonian Institution), Irina Demetradze (Ilia Chavchavadze State University), Tuncay Ercan (Directorate of Mineral Research and Exploration, Turkey), Boris Gasparyan (Institute of Archaeology and Ethnography), Michael Glascock (MURR), Bernard Gratuze (Orléans, France), Leslie Hale (Smithsonian Institution), Albert Harutyunyan (State Engineering University of Armenia), Andrew Kandel (University of Tübingen), Sergey Karapetian (Institute of Geological Sciences, National Academy of Sciences, Armenia), James Luhr (Smithsonian Institution), Givi Maisuradze (Georgian Institute of Geology), Khikmet Makhmudov (Baku State University), Khachatur Meliksetian (Institute of Geological Sciences), Nino Sadradze (Georgian Institute of Geology), Ivan Savov (Leeds University), Robert L. Smith (United States Geological Survey), George "Rip" Rapp (University of Minnesota-Duluth), Bastien Varoutsikos (Harvard University), John Whittaker (Grinnell College), and Zehra Yeğingil (Çukurova University, Turkey). Field support and assistance was provided by (in alphabetical order): Ani Adigyozalyan (Institute for Archaeology and Ethnography, Armenia), Daniel Adler (University of Connecticut), Pavel Avetisyan (Institute for Archaeology

and Ethnography), Hayk Azizbekyan (Yerevan State University), Emily Beverly (University of Houston), Simon Blockley (Royal Holloway, University of London), Alex Brittingham (University of Connecticut), Boris Gasparyan (Institute of Archaeology and Ethnography), Robert Ghukasyan (Timeland), Jayson Gill (University of Connecticut), Phil Glauberman (University of Connecticut), Hayk Haydosyan (Institute of Archaeology and Ethnography), Andrew Kandel (University of Tübingen), Sergey Karapetian (Institute of Geological Sciences), Suren Kesejyan (Gfoeller Renaissance Foundation), Arik Malinsky-Buller (Hebrew University), Christina Manning (Royal Holloway, University of London), Khachatur Meliksetian (Institute of Geological Sciences), Hovik Partevyan and the Partevyan family, Artur Petrosyan (Institute of Archaeology and Ethnography), Katie Preece (Swansea University), Yannick Raczynski-Henk (the world's most interesting man), Beverly Schmidt-Magee (University of Connecticut), Jenni Sherriff (Royal Holloway, University of London), Keith Wilkinson (University of Winchester), and Benik Yeritsyan (Institute of Archaeology and Ethnography). Other research support was provided by (in alphabetical order): Dmitri Arakelyan (Institute of Geological Sciences), Dario Bilardello (Institute for Rock Magnetism), Julie Bowles (Institute for Rock Magnetism), Magen Coleman (MURR), Giselle Conde (University of Wisconsin-Eau Claire), Roger Doonan (University of Sheffield), Josh Feinberg (Institute for Rock Magnetism), Jeff Ferguson (MURR), Jill Ferguson (University of Wisconsin-Eau Claire), Liev Frahm, Sylvie Frahm, Michael Glascock (MURR), Katherine Hayes (University of Minnesota-Twin Cities), Amy Hillis (Macalester College), Phil Ihinger (University of Wisconsin-Eau Claire), Mike Jackson (Institute for Rock Magnetism), Charissa Johnson (University of Minnesota-Twin Cities), Peter McSwiggen (University of Minnesota-Twin Cities), Samvel Nahapetyan (Yerevan State University), Steven Newman (University of Minnesota-Twin Cities), Alex Nyers (NW Research Obsidian Studies Lab), Craig Skinner (NW Research Obsidian Studies Lab), and Peter Sølheid (Institute for Rock Magnetism). I also wish to thank the following organizations and institutions for support over the years: Institute for Archaeology and Ethnography, National Academy of Sciences, Republic of Armenia and the Institute of Geological Sciences, National Academy of Sciences, Republic of Armenia; Gfoeller Renaissance Foundation; Departments of Earth Sciences and Anthropology, University of Minnesota-Twin Cities; Institute for Rock Magnetism, University of Minnesota-Twin Cities; the University of Minnesota's Undergraduate Research Opportunity Program (UROP); the University of Minnesota's Grant-in-Aid of Research, Artistry, and Scholarship Program; Marie Curie Network FP7-PEOPLE-2010-ITN (European Commission): New Archaeological Research Network for Integrating Approaches to Ancient Material Studies (NARNIA) Project; Department of Archaeology, University of Sheffield; Pleistocene Archaeology, Geochronology, and Environment of the Southern Caucasus Project funded by the Leverhulme Trust; Hrazdan Gorge Palaeolithic Project funded by the University of Connecticut and Leakey Foundation; Yale University's Council on Archaeological Studies and Department of Anthropology; and Yale University's Offices of the Vice Provost for Research, Dean of Science, and Dean of Social Science. Two anonymous reviewers provided constructive feedback. To conclude on a personal note, I cannot help but think that, with the database here, this project has come full circle back to its very start. In 1990, George "Rip" Rapp, one of my graduate advisors, joined the University of Tübingen's new excavations at ancient Troy in northwestern Turkey, and the project's director, Manfred Korfmann, asked Rapp to focus on obsidian sourcing. Based on Rapp's earlier work on sourcing native copper, he recognized that the existing databases of obsidian sources and their chemical signatures lacked sufficient rigor – namely, that not all sources had been sampled and that those already sampled had not been so systematically – and, in turn, that a new effort was needed. Therefore, in 1991, Rapp, Tuncay Ercan, and their colleagues visited sources across Turkey and methodically collected more than 900 reference specimens. For complicated reasons, though, most of the specimens sat unanalyzed for more than a decade. During discussions in 2003 and 2004 with Rapp about possible doctoral projects, I learned of this unfinished study. With his support, I took on the project with the intention of completing it as Rapp had initially envisioned in 1990. When, in 2004, Rapp handed the remaining obsidian specimens over to me, along with the sampling maps and field notes, he told me, "Do something great with them," so I am extremely pleased to be able to share all of the resulting data with everyone. Any errors or (mis)interpretations should be considered my own and not those of my colleagues and collaborations over the years.

Appendix A. Supplementary data

Supplementary data to this article can be found online at https://doi.org/10.1016/j.jasrep.2023.104011.

References

Adler, D.S., Wilkinson, K.N., Blockley, S., Mark, D.F., Pinhasi, R., Schmidt-Magee, B.A., Nahapetyan, S., Mallol, C., Berna, F., Glauberman, P.J., Raczynski-Henk, Y., Wales, N., Frahm, E., Jöris, O., MacLeod, A., Smith, V.C., Cullen, V.L., Gasparian, B., 2014. Early Levallois technology and the Lower to Middle Paleolithic transition in the Southern Caucasus. Science 345, 1609–1613. https://doi.org/10.1126/science.1256484.

Adler, D.S., Yeritsyan, B., Wilkinson, K., Pinhasi, R., Bar-Oz, G., Nahapetyan, S., Bailey, R., Schmidt, B.A., Glauberman, P., Wales, N., Gasparian, B., 2012. The Hrazdan Gorge Palaeolithic Project, 2008–2009, in: Archaeology of Armenia in Regional Context. NAS RA Gitutyn Publishing House, Yerevan, pp. 21–37.

Ali, S.H., 2009. Treasures of the earth: need, greed, and a sustainable future. Yale University Press, New Haven.

Anderson, A.T., Davis, A.M., Lu, F., 2000. Evolution of Bishop Tuff Rhyolitic Magma Based on Melt and Magnetite Inclusions and Zoned Phenocrysts. J. Petrol. 41, 449–473. https://doi.org/10.1093/petrology/41.3.449.

Aydar, E., Gourgaud, A., Ulusoy, I., Digonnet, F., Labazuy, P., Sen, E., Bayhan, H., Kurttas, T., Tolluoglu, A.U., 2003. Morphological analysis of active Mount Nemrut stratovolcano, eastern Turkey: evidences and possible impact areas of future eruption. J. Volcanol. Geoth. Res. 123, 301–312. https://doi.org/10.1016/S0377-0273(03)00002-7.

Badalian, R., Bigazzi, G., Cauvin, M.-C., Chataigner, C., Jrbashyan, R., Karapetyan, S.G., Oddone, M., Poidevin, J.-L., 2001. An international research project on Armenian archaeological sites: fission-track dating of obsidians. Radiat. Meas. 34, 373–378. https://doi.org/10.1016/S1350-4487(01)00189-5.

Badalyan, R., Chataigner, C., Kohl, P.L., 2004. Trans-Caucasian Obsidian: The Exploitation of the Sources and their Distribution. A View from the Highlands: Archaeological Studies in Honour of Charles Burney, Ancient Near Eastern Studies. 437–465.

Bellot-Gurlet, L., Bigazzi, G., Dorighel, O., Oddone, M., Poupeau, G., Yeğingil, Z., 1999. The fission-track analysis: An alternative technique for provenance studies of prehistoric obsidian artefacts. Radiat. Meas. 31, 639–644. https://doi.org/10.1016/S1350-4487(99)00157-2.

Biagi, P., Gratuze, B., 2016. New Data on Source Characterization and Exploitation of Obsidian from the Chikiani Area (Georgia). Eurasiatica. Università Ca' Foscari Venezia, Italia https://doi.org/10.14277/6969-093-8/EUR-6-1.

Biagi, P., Nisbet, R., Gratuze, B., 2017. Obsidian mines and their characterization: New aspects of the exploitation of the obsidian sources of Mt. Chikiani (Koyun Dağ) in the Lesser Caucasus of Georgia. The Quarry 12, 2–24.

Bigazzi, G., Poupeau, G., Yeğingil, Z., Bellot-Gurlet, L., 1998. Provenance studies of obsidian artifacts in Anatolia using the fission-track dating method: an overview. L'obsidienne Au Proche et Moyen Orient: Du Volcan à l'outil, BAR International Series. 70–89.

Binder, D., Gratuze, B., Mouralis, D., Balkan-Atlı, N., 2011. New investigations of the Göllüdağ obsidian lava flows system: a multi-disciplinary approach. J. Archaeol. Sci. 38, 3174–3184. https://doi.org/10.1016/j.jas.2011.05.014.

Blackman, M.J., 1984. Provenance Studies of Middle Eastern Obsidian from Sites in Highland Iran. Archaeological Chemistry III, 19–50.

Blackman, M.J., Bishop, R.L., 2007. The Smithsonian-NIST partnership: The application of instrumental neutron activation analysis to archaeology. Archaeometry 49, 321–341. https://doi.org/10.1111/j.1475-4754.2007.00304.x.

Blackman, M.J., Badalian, R., Kikodze, Z., Kohl, P.L., 1998. Chemical Characterization of Caucasian Obsidian Geological Sources., in: L'obsidienne Au Proche et Moyen-Orient: Du Volcan à l'Outil. In: BAR International Series, pp. 205–231.

Borsuk, A.M., 1979. Mezozoyskiye I kaynozoyskiye magmaticheskiye formatcii Bolshogo Kavkaza [Mesozoic and Cenozoic Magmatic Formations of the Greater Caucasus]. Nauka, Moscow.

Bowman, H.R., Asaro, F., Perlman, I., 1973a. Composition variations in obsidian sources and the archaeological implications. Archaeometry 15, 123–127. https://doi.org/10.1111/j.1475-4754.1973.tb00080.x.

Bowman, H.R., Asaro, F., Perlman, I., 1973b. On the Uniformity of Composition in Obsidians and Evidence for Magmatic Mixing. J. Geol. 81, 312–327. https://doi.org/10.1086/627873.

Brennan, P.V., 2000. Obsidian from Volcanic Sequences and Recent Alluvial Deposits, Erzurum District, North-Eastern Anatolia: Chemical Characterisation and

Archaeological Implications. Ancient Near Eastern Studies 128–152. https://doi.org/10.2143/ANES.37.0.1083.
Campbell, S., Healey, E., 2016. Multiple sources: The pXRF analysis of obsidian from Kenan Tepe, S.E. Turkey. Journal of Archaeological Science: Reports 10, 377–389. https://doi.org/10.1016/j.jasrep.2016.10.014.
Campbell, S., Healey, E., Maeda, O., 2020. Profiling an unlocated source: Group 3d obsidian in prehistoric and early historic near East. J. Archaeol. Sci. Rep. 33, 102533 https://doi.org/10.1016/j.jasrep.2020.102533.
Cann, J.R., Renfrew, C., 1964. The Characterization of Obsidian and its application to the Mediterranean Region. Proc. Prehist. Soc. 30, 111–133. https://doi.org/10.1017/S0079497X00015097.
Cauvin, M.-C., 1991. L'obsidienne au Levant Prehistorique: Provenance et Fonction. Cahiers de l'Euphrate 5–6, 163–190.
Cauvin, M.-.-C., Gourgaud, A., Gratuze, B., Arnaud, N.O., Poupeau, G., Poidevin, J.-.-L., Chataigner, C. (Eds.), 1998. L'obsidienne au Proche et Moyen Orient: du volcan à l'outil, BAR international series. Archaeopress, Oxford.
Chataigner, C., Badalian, R., Bigazzi, G., Cauvin, M.-C., Jrbashian, R., Karapetian, S.G., Norelli, P., Oddone, M., Poidevin, J.-L., 2003. Provenance studies of obsidian artefacts from Armenian archaeological sites using the fission-track dating method. J. Non Cryst. Solids 323, 167–171. https://doi.org/10.1016/S0022-3093(03)00300-4.
Chataigner, C., Gratuze, B., 2014. New Data on the Exploitation of Obsidian in the Southern Caucasus (Armenia, Georgia) and Eastern Turkey, Part 1: Source Characterization: Obsidian in the Caucasus (Armenia, Georgia) and eastern Turkey, part 1. Archaeometry 56, 25–47. https://doi.org/10.1111/arcm.12006.
Chataigner, C., Poidevin, J.L., Arnaud, N.O., 1998. Turkish occurrences of obsidian and use by prehistoric peoples in the Near East from 14,000 to 6000 BP. J. Volcanol. Geoth. Res. 85, 517–537. https://doi.org/10.1016/S0377-0273(98)00069-9.
Chataigner, C., Işıklı, M., Gratuze, B., Çil, V., 2014. Obsidian Sources in the Regions of Erzurum and Kars (North-East Turkey): New Data: Obsidian sources in the regions of Erzurum and Kars (north-east Turkey). Archaeometry 56, 351–374. https://doi.org/10.1111/arcm.12002.
Chernyshev, I.V., Lebedev, V.A., Arakelyants, M.M., 2006. K-Ar dating of quaternary volcanics: Methodology and interpretation of results. Petrology 14, 62–80. https://doi.org/10.1134/S0869591106010061.
Cherry, J.F., Faro, E.Z., Minc, L., 2010. Field Survey and Geochemical Characterization of the Southern Armenian Obsidian Sources. J. Field Archaeol. 35, 147–163. https://doi.org/10.1179/009346910X12707321520639.
Çubukçu, H.E., Ulusoy, İ., Aydar, E., Ersoy, O., Şen, E., Gourgaud, A., Guillou, H., 2012. Mt. Nemrut volcano (Eastern Turkey): Temporal petrological evolution. J. Volcanol. Geoth. Res. 209–210, 33–60. https://doi.org/10.1016/j.jvolgeores.2011.08.005.
Dixon, J.E., 1976. Obsidian Characterization Studies in the Mediterranean and Near East. In: Advances in Obsidian Glass Studies: archaeological and geochemical perspectives, edited by R. E. Taylor. Noyes Press, 288–333.
Doronicheva, E.V., Shackley, M.S., 2014. Obsidian Exploitation Strategies in the Middle and Upper Paleolithic of the Northern Caucasus: New Data from Mesmaiskaya Cave. PaleoAnthropology 565–585.
Doronicheva, E.V., Golovanova, L.V., Doronichev, V.B., Shackley, M.S., Nedomolkin, A. G., 2019. New data about exploitation of the Zayukovo (Baksan) obsidian source in Northern Caucasus during the Paleolithic. J. Archaeol. Sci. Rep. 23, 157–165. https://doi.org/10.1016/j.jasrep.2018.10.015.
Eichelberger, J.C., Carrigan, C.R., Westrich, H.R., Price, R.H., 1986. Non-explosive silicic volcanism. Nature 323, 598–602. https://doi.org/10.1038/323598a0.
Ende, M., Schorr, S., Franz, A., Gonzales Aviles, G., Geandier, G., Kloess, G., 2007. Nanocrystals in natural glass. Poster presented in the DGK DGKK Annual Conference, Bremen, Germany.
Ercan, T., Saroglu, F., Kuscu, I., 1995. Features of obsidian beds formed by the activity of the volcanoes in Anatolia since 25 million years B.P., in: The Proceedings of the 29th International Symposium on Archaeometry, 1994 May 9-14, Ankara, Turkey. pp. 505–513.
Fataliyev, R.A., Glascock, M.D., Kuzmin, Y.V., Zeynalov, A.A., 2022. Geological and geochemical characterization of the Kelbadjar (Kechaldag) obsidian source in Azerbaijan, Lesser Caucasus. J. Archaeol. Sci. Rep. 45, 103621 https://doi.org/10.1016/j.jasrep.2022.103621.
Fink, J.H., Manley, C.R., 1987. Origin of pumiceous and glassy textures in rhyolite flows and domes, in: Geological Society of America Special Papers. Geological Society of America, pp. 77–88. https://doi.org/10.1130/SPE212-p77.
Fink, J., 1980. Surface folding and viscosity of rhyolite flows. Geol 8, 250. https://doi.org/10.1130/0091-7613(1980)8<250:SFAVOR>2.0.CO;2.
Fink, J., 1987. The Emplacement of Silicic Domes and Lava Flows, Geological Society of America Special Papers. Geological Society of America. https://doi.org/10.1130/SPE212.
Fornaseri, M., Malpieri, L., Palmieri, A.M., Taddeucci, A., 1975. Analyses of obsidians from the Late Chalcolithic levels of Arslantepe (Malatya). Paléorient 3, 231–246.
Frahm, E., 2012. Distinguishing Nemrut Dağ and Bingöl A obsidians: geochemical and landscape differences and the archaeological implications. J. Archaeol. Sci. 39, 1436–1444. https://doi.org/10.1016/j.jas.2011.12.038.
Frahm, E., 2014. Characterizing obsidian sources with portable XRF: accuracy, reproducibility, and field relationships in a case study from Armenia. J. Archaeol. Sci. 49, 105–125. https://doi.org/10.1016/j.jas.2014.05.003.
Frahm, E., 2019. Introducing the Peabody-Yale Reference Obsidians (PYRO) sets: Open-source calibration and evaluation standards for quantitative X-ray fluorescence analysis. J. Archaeol. Sci. Rep. 27, 101957 https://doi.org/10.1016/j.jasrep.2019.101957.
Frahm, E., 2020. Variation in Nemrut Dağ obsidian at Pre-Pottery Neolithic to Late Bronze Age sites (or: all that's Nemrut Dağ obsidian isn't the Sıcaksu source). J. Archaeol. Sci. Rep. 32, 102438 https://doi.org/10.1016/j.jasrep.2020.102438.
Frahm, E., Brody, L.R., 2019. Origins of obsidian at the "Pompeii of the Syrian Desert:" Sourcing lithic artifacts from the Yale-French excavations at Dura-Europos. J. Archaeol. Sci. Rep. 24, 608–622. https://doi.org/10.1016/j.jasrep.2019.02.024.
Frahm, E., Tryon, C.A., 2019. Origin of an Early Upper Palaeolithic obsidian burin at Ksar Akil (Lebanon): Evidence of increased connectivity ahead of the Levantine Aurignacian? J. Archaeol. Sci. Rep. 28, 102060 https://doi.org/10.1016/j.jasrep.2019.102060.
Frahm, E., Feinberg, J.M., Schmidt-Magee, B.A., Wilkinson, K., Gasparyan, B., Yeritsyan, B., Karapetian, S., Meliksetian, K., Muth, M.J., Adler, D.S., 2014. Sourcing geochemically identical obsidian: multiscalar magnetic variations in the Gutansar volcanic complex and implications for Palaeolithic research in Armenia. J. Archaeol. Sci. 47, 164–178. https://doi.org/10.1016/j.jas.2014.04.015.
Frahm, E., Campbell, S., Healey, E., 2016. Caucasus connections? New data and interpretations for Armenian obsidian in Northern Mesopotamia. J. Archaeol. Sci. Rep. 9, 543–564. https://doi.org/10.1016/j.jasrep.2016.08.023.
Frahm, E., Sherriff, J., Wilkinson, K.N., Beverly, E.J., Adler, D.S., Gasparyan, B., 2017. Ptghni: A new obsidian source in the Hrazdan River basin, Armenia. J. Archaeol. Sci. Rep. 14, 55–64. https://doi.org/10.1016/j.jasrep.2017.05.039.
Frahm, E., Kandel, A.W., Gasparyan, B., 2019. Upper Palaeolithic Settlement and Mobility in the Armenian Highlands: Agent-Based Modeling, Obsidian Sourcing, and Lithic Analysis at Aghitu-3 Cave. J Paleo Arch 2, 418–465. https://doi.org/10.1007/s41982-019-00025-5.
Frahm, E., Owen Jones, C., Corolla, M., Wilkinson, K.N., Sherriff, J.E., Gasparyan, B., Adler, D.S., 2020. Comparing Lower and Middle Palaeolithic lithic procurement behaviors within the Hrazdan basin of central Armenia. J. Archaeol. Sci. Rep. 32, 102389 https://doi.org/10.1016/j.jasrep.2020.102389.
Frahm, E., Martirosyan-Olshansky, K., Sherriff, J.E., Wilkinson, K.N., Glauberman, P., Raczynski-Henk, Y., Gasparyan, B., Adler, D.S., 2021. Geochemical changes in obsidian outcrops with elevation at Hatis volcano (Armenia) and corresponding Lower Palaeolithic artifacts from Nor Geghi 1. J. Archaeol. Sci. Rep. 38, 103097 https://doi.org/10.1016/j.jasrep.2021.103097.
Frahm, E., 2010. The Bronze-Age Obsidian Industry at Tell Mozan (Ancient Urkesh), Syria. Doctoral dissertation, University of Minnesota. https://hdl.handle.net/11299/99753.
Gasparyan, B., Egelend, C., Alder, D.S., Pinhasi, R., Glauberman, P., Haydosyan, H., 2014. The Middle Paleolithic Occupation of Armenia: Summarizing Old and New Data, in: Stone Age of Armenia: A Guide-Book to the Stone Age Archaeology in the Republic of Armenia. Monograph of the JSPS-Bilateral Joint Research Project, Center for Cultural Resource Studies, Kanazawa University.
Glascock, M.D., 2011. Chapter 8: Comparison and Contrast Between XRF and NAA: Used for Characterization Of Obsidian Sources in Central Mexico, in: X-Ray Fluorescence Spectrometry (XRF) in Geoarchaeology. pp. 161–192.
Glauberman, P., Gasparyan, B., Wilkinson, K.N., Frahm, E., Raczynski-Henk, Y., Haydosyan, H., Arakelyan, D., Karapetian, S., Nahapetyan, S., Adler, D.S., 2016. Introducing Barozh 12: A Middle Palaeolithic open-air site on the edge of the Ararat Depression, Armenia. ARAMAZD: Armenian Journal of Near Eastern Studies 9(2), 7–20, 158–174.
Glauberman, P., Gasparyan, B., Sherriff, J., Wilkinson, K., Li, B., Knul, M., Brittingham, A., Hren, M.T., Arakelyan, D., Nahapetyan, S., Raczynski-Henk, Y., Haydosyan, H., Adler, D.S., 2020. Barozh 12: Formation processes of a late Middle Paleolithic open-air site in western Armenia. Quat. Sci. Rev. 236, 106276 https://doi.org/10.1016/j.quascirev.2020.106276.
Gratuze, B., Badalyan, R., Chataigner, C., 2022. The provenance of the obsidian used at Aknashen, in: The Neolithic Settlement of Aknashen (Ararat Valley, Armenia): Excavation Seasons 2004-2015. Archaeopress Publishing, pp. 151–167.
Grebennikov, A.V., Kuzmin, Y.V., 2017. The identification of archaeological obsidian sources on Kamchatka Peninsula (Russian Far East) using geochemical and geological data: Current progress. Quat. Int. 442, 95–103. https://doi.org/10.1016/j.quaint.2016.03.020.
Hancock, R.G.V., Carter, T., 2010. How reliable are our published archaeometric analyses? Effects of analytical techniques through time on the elemental analysis of obsidians. J. Archaeol. Sci. 37, 243–250. https://doi.org/10.1016/j.jas.2009.10.004.
Harbottle, G., 1982. Chemical Characterization in Archaeology. In: Contexts for Prehistoric Exchange. Academic Press, New York, pp. 13–51.
Hess, J.C., Lippolt, H.J., Gurbanov, A.G., Michalski, I., 1993. The cooling history of the late Pliocene Eldzhurtinskiy granite (Caucasus, Russia) and the thermochronological potential of grain-size/age relationships. Earth Planet. Sci. Lett. 117, 393–406. https://doi.org/10.1016/0012-821X(93)90092-N.
Hughes, R.E., 1998. On Reliability, Validity, and Scale in Obsidian Sourcing Research. In: Unit Issues in Archaeology: Measuring Time, Space, and Material. University of Utah Press, pp. 103–114.
Hughes, R.E., Smith, R.L., 1993. Archaeology, geology, and geochemistry in obsidian provenance studies, in: Geological Society of America Special Papers. Geological Society of America, pp. 79–91. https://doi.org/10.1130/SPE283-p79.
Imamverdiyev, N.A., Gasangulieva, M.Y., Babaeva, G.J., Abdullaeva, S.F., Veliev, A.A., 2018. Petrogenesis of the Late Cenozoic collision volcanism in the central part of the Lesser Caucasus (Azerbaijan). Russ. Geol. Geophys. 59, 41–54. https://doi.org/10.1016/j.rgg.2018.01.003.
Innocenti, F., Mazzuoli, R., Pasquarè, G., Radicati Di Brozolo, F., Villari, L., 1976. Evolution of the volcanism in the area of interaction between the arabian, anatolian and iranian plates (Lake van, Eastern Turkey). J. Volcanol. Geoth. Res. 1, 103–112. https://doi.org/10.1016/0377-0273(76)90001-9.

Innocenti, F., Mazzuoli, R., Pasquarè, G., Serri, G., Villari, L., 1980. Geology of the volcanic area north of Lake Van (Turkey). Geol Rund. 69, 292–323.
Innocenti, F., Mazzuoli, R., Pasquarè, G., Radicati Di Brozolo, F., Villari, L., 1982. Tertiary and quaternary volcanism of the Erzurum-Kars area (Eastern Turkey): Geochronological data and geodynamic evolution. J. Volcanol. Geoth. Res. 13, 223–240. https://doi.org/10.1016/0377-0273(82)90052-X.
Kandel, A.W., Gasparyan, B., Bruch, A.A., Weissbrod, L., Zardaryan, D., 2011. Introducing Aghitu-3, the first Upper Paleolithic cave site in Armenia. Armenian J. Near East. Stud. 6, 7–23.
Kandel, A.W., Gasparyan, B., Allué, E., Bigga, G., Bruch, A.A., Cullen, V.L., Frahm, E., Ghukasyan, R., Gruwier, B., Jabbour, F., Miller, C.E., Taller, A., Vardazaryan, V., Vasilyan, D., Weissbrod, L., 2017. The earliest evidence for Upper Paleolithic occupation in the Armenian Highlands at Aghitu-3 Cave. J. Hum. Evol. 110, 37–68. https://doi.org/10.1016/j.jhevol.2017.05.010.
Karaoğlu, Ö., Özdemir, Y., Tolluoğlu, A.Ü., Karabiyikoğlu, M., Köse, O., Froger, J.-L., 2005. Stratigraphy of the volcanic products around Nemrut caldera: Implications for reconstruction of the caldera formation. Turk. J. Earth Sci. 14, 123–143.
Karapetian, S.G., 1969. Geological conditions of the formation of acid volcanic glass deposits in SSR Arm. In: Regularities of formation and location of volcanic glass deposits (in Russian). Nauka, Russia, pp. 38–46.
Karapetian, S.G., Meliksetian, B.M., Shirinian, K.G., Yashvili, L.P., 1986. Mineral composition, geochemical and genetic features of the Bartsratumb deposits of manganese mineralization in Zangezur (in Russian). Izv. Acad. Sci. SSR Armenia, Earth Sci. Sect. XXXIX, 19–30.
Karapetian, S.G., Jrbashian, R.T., Mnatsakanian, A.K., 2001. Late collision rhyolitic volcanism in the north-eastern part of the Armenian Highland. J. Volcanol. Geoth. Res. 112, 189–220. https://doi.org/10.1016/S0377-0273(01)00241-4.
Keller, J., Seifried, C., 1990. The Present Status of Obsidian Source Identification in Anatolia and the Near East, in: PACT 25: Volcanology and Archaeology, Proceedings of the European Workshops of Ravello. pp. 57–87.
Keller, J., Djerbashian, E., Pernicka, E., Karapetian, S., Nasedkin, V., 1996. Armenian and Caucasian Obsidian Occurrences as Sources for the Neolithic Trade: Volcanological Setting and Chemical Characteristics, in: Archaeometry 94: The Proceedings of the 29th International Symposium on Archaeometry; Ankara, 9-14 May 1994. pp. 69–86.
Kloess, G., Schöps, D., Pirrung, M., 2003. The color of obsidian: nano- and microstructural constraints. Poster presented at GEO 2003, Bochum, Germany.
Kobayashi, K., Sagona, A., 2008. A survey of obsidian sources in the provinces of Erzurum, Erzincan, Rize and Bitlis, 2006. Arastirma Sonuçlari Toplantisi 25, 185–196.
Komarov, A.N., Skovorodkin, N.V., Karapetian, S.G., 1972. Determination of the age of natural glasses according to tracks of uranium fission fragments. Geochimia 6, 693–698.
Le Bourdonnec, F.-X., Nomade, S., Poupeau, G., Guillou, H., Tushabramishvili, N., Moncel, M.-H., Pleurdeau, D., Agapishvili, T., Voinchet, P., Mgeladze, A., Lordkipanidze, D., 2012. Multiple origins of Bondi Cave and Ortvale Klde (NW Georgia) obsidians and human mobility in Transcaucasia during the Middle and Upper Palaeolithic. J. Archaeol. Sci. 39, 1317–1330. https://doi.org/10.1016/j.jas.2011.12.008.
Lebedev, V.A., Bubnov, S.N., Dudauri, O.Z., Vashakidze, G.T., 2008. Geochronology of Pliocene volcanism in the Dzhavakheti Highland (the Lesser Caucasus). Part 2: Eastern part of the Dzhavakheti Highland. Regional geological correlation. Stratigr. Geol. Correl. 16, 553–574. https://doi.org/10.1134/S0869593808050080.
Lebedev, V.A., Chernyshev, I.V., Shatagin, K.N., Bubnov, S.N., Yakushev, A.I., 2013. The quaternary volcanic rocks of the Geghama highland, Lesser Caucasus, Armenia: Geochronology, isotopic Sr-Nd characteristics, and origin. J. Volcanolog. Seismol. 7, 204–229. https://doi.org/10.1134/S0742046313030044.
Malinsky-Buller, A., Glauberman, P., Wilkinson, K., Li, B., Frahm, E., Gasparyan, B., Timms, R., Adler, D.S., Sherriff, J., 2021. Evidence for Middle Palaeolithic occupation and landscape change in central Armenia at the open-air site of Alapars-1. Quat. res. 99, 223–247. https://doi.org/10.1017/qua.2020.61.
Marakushev, A.A., Mamedov, A.I., 1993. Trends of variation in the composition of silicic volcanic glasses. Int. Geol. Rev. 35, 146–169. https://doi.org/10.1080/00206819309465519.
Matsuda, J.I., 1990. K-Ar age of Turkey volcanics. Initial report of Turkey-Japan Volcanological Project, Part II.
Matsuda, J.I., 1988. Geochemical study of collision volcanism at the plate boundary in Turkey (comparison with subduction volcanism in Japan), Initial Report of Turkey–Japan Volcanological Project.
Maziar, S., Glascock, M.D., 2017. Communication networks and economical interactions: Sourcing obsidian in the Araxes River basin. J. Archaeol. Sci. Rep. 14, 31–37. https://doi.org/10.1016/j.jasrep.2017.05.021.
Moorey, P.R.S., 1999. Ancient Mesopotamian materials and industries: the archaeological evidence. Eisenbrauns.
Neff, H., 1998. Units in Chemistry-Based Ceramic Provenance Investigations. In: Unit Issues in Archaeology: Measuring Time, Space, and Material. University of Utah Press, pp. 115–127.
Nishiaki, Y., Maeda, O., Kannari, T., Nagai, M., Healey, E., Guliyev, F., Campbell, S., 2019. Obsidian provenance analyses at Göytepe, Azerbaijan: Implications for understanding Neolithic socioeconomies in the southern Caucasus: Obsidian provenance analyses at Göytepe, Azerbaijan. Archaeometry 61, 765–782. https://doi.org/10.1111/arcm.12457.
Nomade, S., Scao, V., Guillou, H., Messager, E., Mgeladze, A., Voinchet, P., Renne, P.R., Courtin-Nomade, A., Bardintzeff, J.M., Ferring, R., Lordkipanidze, D., 2016. New 40Ar/39Ar, unspiked K/Ar and geochemical constraints on the Pleistocene magmatism of the Samtskhe-Javakheti highlands (Republic of Georgia). Quat. Int. 395, 45–59. https://doi.org/10.1016/j.quaint.2015.05.049.
Notsu, K., Fujitani, T., Ui, T., Matsuda, J., Ercan, T., 1995. Geochemical features of collision-related volcanic rocks in central and eastern Anatolia, Turkey. J. Volcanol. Geoth. Res. 64, 171–191. https://doi.org/10.1016/0377-0273(94)00077-T.
Oddone, M., Yegingil, Z., Bigazzi, G., Ercan, T., Özdogan, M., 1997. Chemical characterisations of Anatolian obsidians by instrumental and epithermal neutron activation analysis. J Radioanal Nucl Chem 224, 27–38. https://doi.org/10.1007/BF02034607.
Oddone, M., Bigazzi, G., Keheyan, Y., Meloni, S., 2000. Characterisation of Armenian Obsidians: Implications for Raw Material Supply for Prehistoric Artifacts. J. Radioanal. Nucl. Chem. 243, 673–682. https://doi.org/10.1023/A:1010666118830.
Olshansky, K., 2018. Obsidian Economy in the Armenian Highlands During the Late Neolithic: A View from Masis Blur. University of California-Los Angeles, Institute of Archaeology.
Orange, M., Le Bourdonnec, F.-X., Berthon, R., Mouralis, D., Gratuze, B., Thomalsky, J., Abedi, A., Marro, C., 2021. Extending the scale of obsidian studies: Towards a high-resolution investigation of obsidian prehistoric circulation patterns in the southern Caucasus and north-western Iran. Archaeometry 63, 923–940. https://doi.org/10.1111/arcm.12660.
Özdemir, Y., Karaoğlu, Ö., Tolluoğlu, A.Ü., Güleç, N., 2006. Volcanostratigraphy and petrogenesis of the Nemrut stratovolcano (East Anatolian High Plateau): The most recent post-collisional volcanism in Turkey. Chem. Geol. 226, 189–211. https://doi.org/10.1016/j.chemgeo.2005.09.020.
Palumbi, G., Gratuze, B., Harutyunyan, A., Chataigner, C., 2014. Obsidian-tempered pottery in the Southern Caucasus: a new approach to obsidian as a ceramic-temper. J. Archaeol. Sci. 44, 43–54. https://doi.org/10.1016/j.jas.2014.01.017.
Palumbi, G., Guilbeau, D., Astruc, L., Chataigner, C., Gratuze, B., Lyonnet, B., Pulitani, G., 2018. Between cooking and knapping in the southern Caucasus: Obsidian-tempered ceramics from Aratashen (Armenia) and Mentesh Tepe (Azerbaijan). Quat. Int. 468, 121–133. https://doi.org/10.1016/j.quaint.2017.10.005.
Pasquarè, G., 1971. Cenozoic volcanics of the Erzurum area (Turkish Armenia). Geol Rundsch 60, 900–911. https://doi.org/10.1007/BF02046527.
Pearce, J.A., Bender, J.F., De Long, S.E., Kidd, W.S.F., Low, P.J., Güner, Y., Saroglu, F., Yilmaz, Y., Moorbath, S., Mitchell, J.G., 1990. Genesis of collision volcanism in Eastern Anatolia, Turkey. J. Volcanol. Geoth. Res. 44, 189–229. https://doi.org/10.1016/0377-0273(90)90018-B.
Poidevin, J.-L., 1998. Les Gisements d'Obsidienne de Turquie et de Transcaucasie: Géologie, Géochimie et Chronométrie, in: L'obsidienne Au Proche et Moyen-Orient: Du Volcan à l'Outil. British Archaeological Reports, pp. 105–167.
Poupeau, G., Le Bourdonnec, F.-X., Carter, T., Delerue, S., Steven Shackley, M., Barrat, J.-A., Dubernet, S., Moretto, P., Calligaro, T., Milić, M., Kobayashi, K., 2010. The use of SEM-EDS, PIXE and EDXRF for obsidian provenance studies in the Near East: a case study from Neolithic Çatalhöyük (central Anatolia). J. Archaeol. Sci. 37, 2705–2720. https://doi.org/10.1016/j.jas.2010.06.007.
Renfrew, C., Cann, J.R., Dixon, J.E., 1965. Obsidian in the Aegean. Annu. Br. Sch. Athens 60, 225–247. https://doi.org/10.1017/S0068245400013976.
Renfrew, C., Dixon, J.E., 1976. Obsidian in Western Asia: A Review. Problems in Economics and Social Archaeology 42, 137–150.
Renfrew, C., Dixon, J.E., Cann, J.R., 1966. Obsidian and Early Cultural Contact in the Near East. Proc. Prehist. Soc. 32, 30–72. https://doi.org/10.1017/S0079497X0001433X.
Renfrew, C., Dixon, J., Cann, J., 1969. Further Analysis of Near Eastern Obsidians. Proc. Prehist. Soc 34, 319–331. https://doi.org/10.1017/S0079497X0001392X.
Robin, A.-K., Mouralis, D., Kuzucuoğlu, C., Akköprü, E., Gratuze, B., Doğu, A.F., Erturaç, K., Cétoute, J., 2015. Les affleurements d'obsidiennes du Nemrut (Anatolie orientale): mise en évidence d'une source exploitable, premiers résultats. geomorphologie 21, 217–234. https://doi.org/10.4000/geomorphologie.11055.
Robin, A.K., Mouralis, D., Akköprü, E., Gratuze, B., Kuzucuoğlu, C., Nomade, S., Pereira, A., Doğu, A.F., Erturaç, K., Khalidi, L., 2016. Identification and characterization of two new obsidian sub-sources in the Nemrut volcano (Eastern Anatolia, Turkey): The Sıcaksu and Kayacık obsidian. J. Archaeol. Sci. Rep. 9, 705–717. https://doi.org/10.1016/j.jasrep.2016.08.048.
Shackley, M.S., Doronicheva, E.V., Doronichev, V.B., Golovanova, L.V., Nesmeyanov, S.A., Voeykova, O.A., Muriy, A.A., 2018. The Zayukovo (Baksan) archaeological obsidian source, Greater Caucasus, Russia. IAOS Bulletin 60, 11–23.
Shalaeva, E.A., Trifonov, V.G., Lebedev, V.A., Simakova, A.N., Avagyan, A.V., Sahakyan, L.H., Arakelyan, D.G., Sokolov, S.A., Bachmanov, D.M., Kolesnichenko, A.A., Latyshev, A.V., Belyaeva, E.V., Lyubin, V.P., Frolov, P.D., Tesakov, A.S., Sychevskaya, E.K., Kovalyova, G.V., Martirosyan, M., Khisamutdinova, A.I., 2019. Quaternary geology and origin of the Shirak Basin, NW Armenia. Quat. Int. 509, 41–61. https://doi.org/10.1016/j.quaint.2018.09.017.
Sharkov, E., Lebedev, V., Chugaev, A., Zabarinskaya, L., Rodnikov, A., Sergeeva, N., Safonova, I., 2015. The Caucasian-Arabian segment of the Alpine-Himalayan collisional belt: Geology, volcanism and neotectonics. Geosci. Front. 6, 513–522. https://doi.org/10.1016/j.gsf.2014.07.001.
Sherriff, J.E., Wilkinson, K.N., Adler, D.S., Arakelyan, D., Beverly, E.J., Blockley, S.P.E., Gasparyan, B., Mark, D.F., Meliksetian, K., Nahapetyan, S., Preece, K.J., Timms, R.G.O., 2019. Pleistocene volcanism and the geomorphological record of the Hrazdan valley, central Armenia: linking landscape dynamics and the Palaeolithic record. Quat. Sci. Rev. 226, 105994 https://doi.org/10.1016/j.quascirev.2019.105994.
Shirinian, K.G., Karapetian, S.G., 1964. Specific features in the structure and petrology of rhyolithic dome-shaped volcanoes of Armenia. Bull Volcanol 27, 25–27. https://doi.org/10.1007/BF02597504.

Sugden, P., Meliksetian, K., Savov, I.P., Barfod, D., Wilson, M., Connor, C., Navasardyan, G., Grigoryan, E., Manucharyan, D., 2021. Post-collisional shift from polygenetic to monogenetic volcanism revealed by new 40Ar/39Ar ages in the southern Lesser Caucasus (Armenia). J. Volcanol. Geoth. Res. 412, 107192 https://doi.org/10.1016/j.jvolgeores.2021.107192.

Todd, I.A., 1980. The Prehistory of Central Anatolia I: The Neolithic Period. Åström.

Trifonov, V.G., Shalaeva, E.A., Saakyan, L.Kh., Bachmanov, D.M., Lebedev, V.A., Trikhunkov, Ya.I., Simakova, A.N., Avagyan, A.V., Tesakov, A.S., Frolov, P.D., Lyubin, V.P., Belyaeva, E.V., Latyshev, A.V., Ozherelyev, D.V., Kolesnichenko, A.A., 2017. Quaternary tectonics of recent basins in northwestern Armenia. Geotecton. 51, 499–519. https://doi.org/10.1134/S0016852117030116.

Ulusoy, İ., Çubukçu, H.E., Mouralis, D., Aydar, E., 2019. Nemrut caldera and Eastern Anatolian volcanoes: Fire in the highlands. In: In: Landscapes and Landforms of Turkey, pp. 589–599.

Wagner, G.A., Weiner, K.L., 1987. Deutches Archaeologisches Institut Demircihoyuk. Die Ergebenisse des Ausgrabungen 1975–1978. Herausgegeben von Manfred Korfmann Band II: Naturwissenschaftliche Untersuchungen. Verlag Philipp von Zabern, Mainz, Germany, pp. 26–29.

Wagner, G.A., Storzer, D., Keller, J., 1976. Spaltspurendatierung quartärer Gesteinsgläser aus dem Mittelmeerraum. Neues Jahrb. filr Mineral. Monatsh. 2, 84–94.

Weiss, S., Kloess, G., Schöps, D., Kletti, H., Sandiklar, B., Heide, K., 2002. Density and composition map of the massive Ikizdere obsidian flow, East Pontides. Turkey, Natural Glasses, Lyon, France.

Wilson, L., Pollard, A.M., 2001. The Provenance Hypothesis. In: Handbook of Archaeological Sciences. John Wiley and Sons, pp. 507-517.

Yeğingil, Z., Boztug, D., Er, M., Oddone, M., Bigazzi, G., 2002. Timing of neotectonic fracturing by fission track dating of obsidian in-filling faults in the Ikizdere-Rize area, NE Black Sea region, Turkey. Terra Nova 14, 169–174. https://doi.org/10.1046/j.1365-3121.2002.00407.x.

Yellin, J., Perlman, I., 1981. Source obsidian rare earth patterns and obsidian artefact provenience. arsci 1, 325–330. https://doi.org/10.3406/arsci.1981.1163.

Yilmaz, Y., Şaroğlu, F., Güner, Y., 1987. Initiation of the neomagmatism in East Anatolia. Tectonophysics 134, 177–199. https://doi.org/10.1016/0040-1951(87)90256-3.

Yilmaz, Y., Güner, Y., Şaroğlu, F., 1998. Geology of the quaternary volcanic centres of the east Anatolia. J. Volcanol. Geoth. Res. 85, 173–210. https://doi.org/10.1016/S0377-0273(98)00055-9.